APPENDIX 3A

COMPUTER PROGRAMS USED IN STRUCTURAL ANALYSIS AND DESIGN

INDEX

APPENDIX 3A

COMPUTER PROGRAMS USED IN STRUCTURAL ANALYSIS AND DESIGN

3A.1 ASHSD (AXISYMMETRIC SHELL AND SOLID)

3A.1.1 Description

ASHSD is a special purpose program that can be used in the elastic, static, or dynamic analysis of structural systems capable of being represented as axisymmetric shells and/or solids.

This program allows study of the interaction between a typical nuclear containment structure, modeled as an axisymmetric shell, and the subsoil, modeled as an axisymmetric solid. It is a refinement of the original ASHSD program developed at the University of California at Berkeley. The present program is highly modified for static and dynamic analysis of nuclear containment structures. The modified program has the following features:

1. A shell finite element that uses an interaction stiffness, allowing analysis of layered shells.

2. Because shell layers may be bonded or unbonded from each other, it is possible to describe concrete shells in their geometric form. For example, it is possible to describe liner plate, concrete, and reinforcing steel, in their real spatial locations.

3. Isotropic or orthotropic elastic constants are possible for both shell and solid elements. The orthotropic material properties may be used to describe the different stiffnesses of reinforcing steel, e.g., in the hoop and meridional directions.

4. Nonuniform thermal gradients through the wall thickness may be imposed.

5. Eigenvalues and eigenvectors may be computed.

6. Three dynamic response routines are available in the program:

   a. Arbitrary dynamic loading, or earthquake based excitation using an uncoupled (modal) technique

   b. Arbitrary dynamic loading, or earthquake based excitation using a coupled (direct integration) technique

   c. Response spectrum modal analysis for absolute and square root of the sum of the squares displacements and element stresses

7. The coupled time history solution has the capability to allow an arbitrary damping matrix

8. The stiffness and mass matrices may be obtained as punched output for use in other programs.

The version currently used by Bechtel is maintained by the Control Data Corporation. See Table 3A-1 for program verification information.

3A.2 FINEL (FINITE-ELEMENT PROGRAM FOR CRACKING ANALYSIS)

3A.2.1 Description

This program performs a static analysis of stresses and strains in plane and axisymmetric structures by the finite element method. The program computes the displacements of the corners of each element, and the stresses and strains within each element.

In this program, the structure is idealized as an assemblage of two dimensional finite elements of triangular or quadrilateral shapes, having arbitrary material properties. Reinforcement of concrete materials is included by adjusting the element material properties. Bilinearity in compression, and bilinearity or cracking in tension are especially emphasized.

The version of this program currently used by Bechtel is maintained by the Control Data Corporation. For program verification information, see Table 3A-1.

3A.3 BSAP (BECHTEL STRUCTURAL ANALYSIS PROGRAM)

3A.3.1 Description

The Bechtel structural analysis program (BSAP) is a finite element computer program that is used to perform linear, elastic analyses of three dimensional structural systems. BSAP is an improved version of SAP, a recognized computer program in the public domain, which was originally developed by Dr. E. L. Wilson and his associates at the University of California at Berkeley. For program verification information, see Table 3A-1. This computer program uses the direct stiffness approach. Applications may be simple simulations involving one or two modeling elements, or they may be large and complex simulations. The program is capable of performing static analysis, modal extractions, and dynamic steady state, time history, or spectral response analyses on structures composed of any combination of the following modeling elements:

1. Boundary element (BOUND)

2. Truss element (TRUSS)

3. Beam element (BEAM)

4. Curved beam element (CURVE)

5. Membrane (plane stress) element (MEMB)

6. Simple plate element (SIMP)

7. Shell element (PLATE or LCCT9)

8. Thick shell element (THICK)

9. Brick element (BRICK)

10. Plane strain element (PLANE)

11. Axisymmetric ring element (RING)

12. General element (GENRL).

BSAP includes the following features:

1. Analysis capabilities - Static analysis, eigenvalue analysis, and dynamic response calculations using the modal approach.

   a. Eigenvalue solution algorithms include:

      1. Ritz reduction with Jacobi eigenvalue solution

      2. Kinematic reduction with HQR eigenvalue solution

      3. Determinant search eigenvalue solution

      4. Subspace iteration eigenvalue solution.

   b. Dynamic response calculations include:

      1. Composite modal damping (strain energy approach)

      2. Response spectrum analysis

3. Time history analysis

4. Steady state analysis.

2. Input processor capabilities:

a. Extensive data checking (data editor)

b. Extensive data generation

c. Geometry plotting.

3. Other features:

a. Static load combinations

b. Beam selective output

c. Checkpoint/restart

d. Selective output controls

e. Constraint equations

f. Constant bandwidth or profile storage techniques.

3A.4 ICES/STRUDL-II (STRUCTURAL DESIGN LANGUAGE)

3A.4.1 Description

The ICES/STRUDL-II program is a subsystem of the Integrated Civil Engineering System (ICES), which is a series of problem oriented computer programs written at the Massachusetts Institute of Technology. For program verification information, see Table 3A-1.

The ICES/STRUDL-II program is a finite element computer program that is used to perform linear, elastic analyses of three dimensional structural systems. Applications may be simple simulations involving one or two modeling elements, or they may be large and complex simulations. The program is capable of performing static analysis, modal extractions, and dynamic steady state, time history, or spectral-response analyses on structures composed of any combination of the following modeling elements:

1. Boundary
2. Truss
3. Beam
4. Plane strain
5. Plane stress (membrane)
6. Plate bending (triangular and quadrangular)
7. Bending (triangular)
8. Shallow shell (triangular and rectangular)
9. Tridimensional (brick).

3A.5 STARDYNE

3A.5.1 Description

STARDYNE is a large scale, finite element program that has a broad range of analysis types and many different structural elements. The STARDYNE system of structural analysis programs is segmented into individual programs. A variety of static or dynamic analyses may be performed by using one or more of the individual programs in a coordinated series of computer runs.

This program is used for the static and dynamic analyses of two or three dimensional structural models.

STARDYNE is written and maintained by the System Development Corporation of Santa Monica, California and is available on the Control Data Corporation system. For program verification information, see Table 3A-1.

3A.6 BOSOR4

3A.6.1 Description

BOSOR4 is a computer program for the analysis of the stress, stability, and vibration of segmented shells of revolution, and prismatic shells. BOSOR4 is written and maintained by David Bushnell of the Lockheed Missile and Space Company of Palo Alto, California. The program is designed primarily for vibration buckling, nonlinear, and nonsymmetric stress problems. BOSOR4 has two analysis methods: finite difference energy minimization for the linear problems, and Newton's method for solution of the nonlinear problems. The loading in BOSOR4 may be axisymmetric or nonaxisymmetric, but both must be static.

BOSOR4 is used for the stress and stability analysis of shells of revolution with axisymmetric or nonaxisymmetric static loads. For program verification information, see Table 3A-1.

3A.7 ANSYS

3A.7.1 Description

The ANSYS engineering analysis system computer program is a large scale, general purpose computer program employing finite element technology for the solution of several classes of engineering analysis problems. Analysis capabilities include static and dynamic; plastic, creep, and swelling; small and large deflections; steady state and transient heat transfer; and

steady state fluid flow. A variety of finite elements are available for use in the program. Structural loadings may be forces, displacements, pressures, temperatures, or response spectra. The program output includes joint displacements, and element stresses, forces and moments.

ANSYS was developed by Swanson Analysis Systems, Inc, and is in the public domain. The program is used for linear and non-linear static and dynamic analyses of general structures, non-linear collapse analysis, soil/structure interaction, etc. For program verification information, see Table 3A-1.

3A.8 EDSGAP

3A.8.1 Description

EDS Nuclear program EDSGAP is a general purpose, finite element program for linear, elastic analysis of arbitrary structural systems. EDSGAP is based on the program SAP, developed by Dr. E. L. Wilson at the University of California, at Berkeley, and includes improvements and features of his later version, SAP IV. In addition to input and output options added by EDS for user convenience, considerable effort has gone into increasing the speed and storage capabilities, debugging the various subroutines, and adding analysis features.

The program contains the following element types:

1. General beam
2. Truss
3. Two dimensional plane stress/plane strain
4. Three dimensional solid
5. Axisymmetric solid

6. Plate and shell

7. Translational/rotational spring

8. Fluid.

These element types may be used both singly or in compatible combinations. The program includes static and dynamic options, as discussed below. Out-of-core storage may be used for solving the equations of equilibrium, storing problem data, and storing solution results. The program has virtually no restrictions on size of the structural system that can be analyzed.

Static analyses are performed using the direct stiffness method, in which element stiffness matrices are formed according to virtual work principles and assembled to form a global stiffness matrix for the system, relating external forces and moments to joint displacements and rotations. Applied static loads may be specified as combinations of concentrated forces, thermal expansion loads, pressure forces, and inertia (body) forces. The equations of equilibrium of the system are solved for joint displacements and rotations by Gaussian reduction techniques.

Dynamic options within the program include;

1. Frequency calculations only, by either the Rayleigh Ritz Method or the Generalized Eigenvalue Method

2. Frequency calculations followed by response history analysis by mode superposition

3. Frequency calculations followed by response spectrum analysis

4. Response history analysis by direct integration.

Dynamic loadings may be specified as acceleration spectra, or combinations of arbitrary applied force and moment time histories, and three independent orthogonal component time histories of acceleration.

The basis for EDSGAP is the program SAP, which is an accepted, standard program in the public domain. Nevertheless, EDSGAP has been verified for a comprehensive set of example problems in accordance with the EDS Nuclear Inc quality assurance program. Extensive and complete documentation, with detailed descriptions of the example problems and comparison results from standard programs, or from hand calculations, exists and is available for inspection at the offices of EDS Nuclear Inc in San Francisco.

3A.9 DECON

3A.9.1 Description

The EDS Nuclear Program DECON determines the unique input acceleration time history required at support locations to produce a specified acceleration response time history at any other given location in an arbitrary, two-dimensional structural system. Both the unknown input motion and the specified response time history may include components of motion in two orthogonal directions simultaneously.

The procedure used, known as deconvolution, is based on the replacement of the uncoupled modal differential equations of motion of the structural system by Fourier transform products. The natural modes of vibration of the structural system are used by DECON to generate a frequency dependent transfer function for each mode of the system. These transfer functions are calculated from the steady state harmonic response of the uncoupled modes to all input frequencies in the frequency range of interest, and relate the Fourier components of the specified response time history to the Fourier components of the unknown input motion. The program DECON computes the Fourier transform of the specified motion, uses

the transfer functions of the structural system to compute the Fourier transform to the desired input motion, and performs an inverse Fourier transform to obtain the unknown input accelerations time history.

The program has been verified according to the EDS Nuclear Inc quality assurance program, and complete documentation, including example problems and comparison with theoretical solutions, is available for inspection at the offices of EDS Nuclear Inc in San Francisco.

3A.10 RESPEC

3A.10.1 Description

RESPEC is a special purpose program for computation of response spectra of acceleration time histories. Spectral accelerations are computed for frequencies and damping ratios selected by the user. Each spectra value is obtained by computing the maximum response of a damped, single degree of freedom oscillator subject to the specified acceleration time history. The response is computed by explicit integration of the differential equations of motion, assuming "at rest" initial conditions. The program may also be used to compute the associated velocity and displacement time histories by numerical integration of the specified acceleration record.

The program has been verified for a set of sample problems by comparison with theoretical solutions, published results, and results from other programs, in accordance with the EDS Nuclear Inc quality assurance program.

3A.11 FLUSH

3A.11.1 Description

The program uses finite element techniques to analyze soil structure interaction effects during earthquakes especially for embedded structures. The program provides consideration of variations of ground motion with depth in the soil structure response and deconvolution evaluations. Some of the special features of the program include:

1. Plain strain quadrilateral elements for modeling of soils and structures.

2. Beam elements for modeling of structures

3. Multiple nonlinear soil properties for equivalent linear analysis

4. An approximate three dimensional ability using viscous boundary conditions

5. Generates output time histories of acceleration, bending moment and axial force

6. Computation of maximum shear forces, axial forces, moments and absolute acceleration in beam elements

7. Generates acceleration and velocity response spectra.

The program was developed as Report No. EERC 75-30 at the College of Engineering, University of California, Berkeley, California by J. Lysmer, T. Udaka, C.F. Tsai, and H.B. Seed.

The program is a recognized program in the public domain and has had sufficient history of use to justify its applicability and validity. Document traceability is available at United Information Services, Inc. San Francisco Office.

3A.12 CE 917, MODAL PROPERTIES OF STRUCTURES

3A.12.1 Description

The program computes the reduced stiffness matric from the basic geometry input for plane frame or truss models, or accepts the reduced stiffness matrix for any structure as input. It calculates mode shapes, frequencies, participation factors, and modal damping values for a lumped mass model.

Special Features:

1. Can accept either diagonal or full mass matrices.

2. Generates output tape for input to Bechtel CE 920 and Bechtel CE 931.

The program verification document is available at Bechtel Power Corporation.

3A.13 CE 920, RESPONSE TIME HISTORY

3A.13.1 Description

The program performs the earthquake response time history analysis of lumped mass models, using modal superposition. Program input consists of frequencies, mode shapes, modal damping, and the base acceleration time history. The program calculates and prints out the response time histories of relative displacement, relative

velocity, relative acceleration and absolution acceleration, and the maximum values of inertia forces, shear and moment. The CE 917 output files which contain the modal properties of the system may be used as input to this program.

The program verification document is available at Bechtel Power Corporation.

3A.14 CE 921, RESPONSE SPECTRA

3A.14.1 Description

The program calculates response acceleration, velocity, and displacement spectra for a specified acceleration time history. It can produce printed plots of the calculated response spectra.

The CE 920 output files which contain acceleration time histories may be used as input to this program.

The program verification document is available at Bechtel Power Corporation.

3A.15 CE 931, SOIL-STRUCTURE INTERACTION

3A.15.1 Description

The program computes the frequencies, mode shapes, and composite modal damping values of a lumped soil structure system for seismic analysis. The major input to this program includes the modal frequencies, modal damping and mode shapes, of the fixed-base structures and the foundation soil properties, i.e., equipment foundation springs and dampers. The method for calculating the composite modal damping is discussed in Reference 3.7-1.

Special features:

1. Input may consist of output tape from the Bechtel CE-917 program or direct input of fixed base structural properties.

2. Can be used for either horizontal or vertical seismic analysis.

The program verification document is available at Bechtel Power Corporation.

3A.16 SAFE (INTEGRATED ANALYSIS AND DESIGN OF SLAB SYSTEMS)

3A.16.1 Description

SAFE has been obtained from Computers and Structures, Inc. (CSI), Berkeley, California and installed at Sargent & Lundy LLC. SAFE provides analysis and design tools available for the concrete slabs, such as flat slab, flat slab with perimeter beams, basemats (slab on soil subgrade), spread footings, foundation uplift, slab reinforcing calculated based on user-defined design strips and several other slab related analysis/design. SAFE uses ACI design code for reinforced concrete design.

The verification document of the program is available at Sargent & Lundy LLC (Date: 10-30-2000).

3A.17 RSG (RESPONSE SPECTRUM GENERATOR)

3A.17.1 Description

RSG is developed by Sargent & Lundy LLC. The program has the following features:

1. Generate response spectrum from an input acceleration time history.
2. Envelop response spectra.
3. Combine response spectra by square-root-sum of squares (SRSS) method.
4. Combine response spectra by Absolute Sum Method.
5. Generate spectrum according to ASME Pressure Vessel Research Committee (PVRC) guidelines.
6. Generate a spectrum-consistent acceleration time history (a time history with response spectrum that envelopes a specified spectrum).
7. Plotting and peak widening of response spectrum.

For generating response spectrum from an input acceleration time history, the program uses Newmark's β-method of integration (with β equal to 1/6) to solve the equation of motion of a single-degree of freedom damped oscillator subjected to a base excitation.

The verification document of the program is available at Sargent & Lundy LLC (Date: 11-11-1992).

3A.18 SHAKE (SOIL LAYER PROPERTIES AND RESPONSE / EARTHQUAKE

3A.18.1 Description

John Lysmer and P. B. Schnabel of the University of California, Berkeley, developed the SHAKE program. It was obtained by Sargent & Lundy LLC from the University of California, Berkeley in 1972.

The program computes response in a horizontally layered semi-infinite system subjected to vertically traveling shear waves. Strain dependent soil properties are computed within the program. An earthquake motion can be specified at any level of the soil profile. The method is based on the continuous solution of shear wave equations.

The input includes data for soil profile including half space, curves of strain vs. shear modulus parameters and damping values for the soil types present in the soil profile and the input earthquake motion. The output includes the strain-dependent soil properties at each iteration; response spectrum of object and computed motions. Fourier spectra and response spectra of input, object and computed motions can be obtained.

The verification document of the program is available at Sargent & Lundy LLC (Date: 11-16-1992).

3A.19 SASSI 2000 (A SYSTEM FOR ANALYSIS OF SOIL-STRUCTURE INTERACTION)

3A.19.1 Description

SASSI 2000 consists of a number of integrated computer-program modules, which can be used to solve a wide range of dynamic soil-structure interaction problems in two or three dimensions. The program has the following capabilities:

1. The site consists of semi-infinite elastic or viscoelastic horizontal layers on a rigid base or semi-infinite elastic or viscoelastic halfspace.
2. The structure(s) are idealized by standard two- or three-dimensional finite elements connected at nodal points.
3. Each nodal point on the structure may have up to six displacement degrees of freedom.
4. The excavated soil zone(s) are idealized by standard plane strain or three-dimensional solid elements. The finite element models of the structure and excavated soil have common nodes at the boundary.
5. Earthquake excitation is defined by a time history of acceleration called control motion. The control motion is assigned to one of the three global directions at the control point which lies on a soil layer interface.
6. Transient input time histories are handled by the Fast Fourier Transform technique.
7. Finite element library consists of the following element types:
    a. Three-dimensional solid elements (eight-node brick).
    b. Three-dimensional beam elements.
    c. Four-node quadrilateral plate/shell elements.
    d. Two-dimensional four-node plane strain finite elements.
    e. Three-dimensional spring elements.
    f. Three-dimensional stiffness/mass matrix element.

The basic methods of analysis adopted by the computer program SASSI 2000 are called the flexible volume and subtraction methods. These methods are formulated in the frequency domain using the complex response method and finite element technique. The analytical method used in the SASSI program is restricted to linear analysis. However, approximate nonlinear analysis can be performed by an iterative scheme called "Equivalent Linear Method".

The verification document of the program is available at Sargent & Lundy LLC (Date: 12-28-2001).

3A.20 MSC.VISUALNASTRAN DESKTOP, VERSION 2003/2004

3A.20.1 Description

"VisualNastran" (2003/2004) is a Computer Aided Engineering (CAE) tool with an integrated user interface that merges modeling, simulation, viewing and measuring.

The program includes a dynamic algorithm that provides automatic collision and contact handling, including detection, response, restitution, and friction.

Numerical integration is performed using the Kutta-Merson integrator, which offers options for variable or fixed time-step and error bounding.

The visualNastran Code is commercially available. Holtec has performed independent QA validation of the code (in accordance with Holtec's QA requirements) by comparing the solution of several classical dynamics problems with the numerical results predicted by visualNastran. Agreement in all cases is excellent.

3A.21 SIMULATION OF EARTHQUAKE GROUND MOTIONS. SIMQKE/GENEQ

3A.21.1 Description

Simulation of Earthquake Ground Motions. SIMQKE generates statistically independent accelerograms, performs a baseline correlation on the generated motions to ensure zero final ground velocity, and calculates response spectra. One of the options in the program generates ground motions whose response spectra "match", or are compatible with, a set of specified smooth response spectra. The basis for the spectrum compatible motion generation is the relationship between the response spectrum values for arbitrary damping and the "expected" Fourier amplitudes of the ground motion (Vanmarcke, 1976). The earthquakes are synthesized by superimposing sinusoidal components with pseudo-random phase angles, and by multiplying the resulting stationary trace by a user specified function representing the variation of ground motion intensity with time. The program also has the capability to adjust, by iteration, the ordinates of the spectral density function to improve the agreement between the computed and specified response spectra. Even without the last step, the average response spectrum (of a set of simulated motions) will match the smooth target spectrum very closely. GENEQ is a modified version of this software for PC systems with the following additional features:

1. Input spectrum can be amplified by a user-specified scale factor to improve enveloping of target spectrum;
2. Output files have been expanded to include power spectral density (PSD) data.

TABLE 3A-1

PROGRAM VERIFICATION DATA

Program			Version	Documentation Status		FSAR
No.	Acronym	Description	Date	Verification Report	Location of Verification Document	Reference Section
CE798	ANSYS	General finite element analysis	3A 11/15/78	Complete	CDC/SF office	3.8.2
			A8/67J 4/21/80	Complete	Bechtel/SF office	
CE800	BSAP	General finite element analysis	D15/34 02/12/81	Complete	Bechtel/SF office	3.8.4 and 3.8.5
			D14/33 12/10/80	Complete	Bechtel/SF office	
			D13/32 11/21/80	Complete	Bechtel/SF office	
			D12/31 10/29/80	Complete	Bechtel/SF office	
			D11/30 10/24/80	Complete	Bechtel SF office	
			D10/29 10/1/80	Complete	Bechtel/SF office	
			D9 9/16/80	Complete	Bechtel/SF office	
			D8 8/15/80	Complete	Bechtel/SF office	
			D7 7/31/80	Complete	Bechtel/SF office	
			D6 6/26/80	Complete	Bechtel/SF office	
			D5 6/19/80	Complete	Bechtel/SF office	
			D4 5/23/80	Complete	Bechtel/SF office	

TABLE 3A-1 (Cont)

Program			Documentation Status			
No.	Acronym	Description	Version Date	Verification Report	Location of Verification Document	FSAR Reference Section
CE800	BSAP (cont)	General finite element analysis	D3 5/1/80	Complete	Bechtel/SF office	
			D2 4/11/80	Complete	Bechtel/SF office	
			D1 3/28/80	Complete	Bechtel/SF office	
			C17 07/03/79	Complete	Bechtel/SF office	
			C16 03/21/79	Complete	Bechtel/SF office	
			C15 02/15/79	Complete	Bechtel/SF office	
			C14A 12/21/78	Complete	Bechtel/SF office	
			C14 04/03/78	Complete	Bechtel/SF office	
			C13 02/03/78	Complete	Bechtel/SF office	
			C12 01/18/78	Complete	Bechtel/SF office	
			C11 12/28/77	Complete	Bechtel/SF office	
			C10 10/31/77	Complete	Bechtel/SF office	
			C9 08/15/77	Complete	Bechtel/SF office	
			C8 06/21/77	Complete	Bechtel/SF office	
			C7 06/03/77	Complete	Bechtel/SF office	

TABLE 3A-1 (Cont)

Program			Documentation Status			
No.	Acronym	Description	Version Date	Verification Report	Location of Verification Document	FSAR Reference Section
CE800	BSAP (cont)	General finite element analysis	D15/34 02/19/81	Complete	Bechtel/AL office	
			D14/33 12/22/80	Complete	Bechtel/LA office	
			D13/32 11/29/80	Complete	Bechtel/LA office	
			D12/31 10/28/80	Complete	Bechtel/LA office	
			D11/30 10/24/80	Complete	Bechtel/LA office	
			D10/29 10/1/80	Complete	Bechtel/LA office	
			D9 9/16/80	Complete	Bechtel/LA office	
			D8 8/15/80	Complete	Bechtel/LA office	
			D7 7/31/80	Complete	Bechtel/LA office	
			D6 6/26/80	Complete	Bechtel/LA office	
			D5 6/19/80	Complete	Bechtel/LA office	
			D4 5/23/80	Complete	Bechtel/LA office	
			D3 5/1/80	Complete	Bechtel/LA office	
			D2 4/11/80	Complete	Bechtel/LA office	
			D1 3/28/80	Complete	Bechtel/LA office	

TABLE 3A-1 (Cont)

Program			Version	Documentation Status		FSAR
No.	Acronym	Description	Date	Verification Report	Location of Verification Document	Reference Section
CE800	BSAP (cont)	General finite element analysis	C17 07/31/79	Complete	Bechtel/SF office	
			C16 03/21/79	Complete	Bechtel/SF office	
			C15 02/15/79	Complete	Bechtel/SF office	
			C14A 12/12/78	Complete	Bechtel/SF office	
			C14 04/03/78	Complete	Bechtel/SF office	
			C13 02/03/78	Complete	Bechtel/SF office	
			C12 01/18/77	Complete	Bechtel/SF office	
			C11 12/78/77	Complete	Bechtel/SF office	
			C10 10/31/77	Complete	Bechtel/SF office	
			C9 08/15/77	Complete	Bechtel/SF office	
			C8 06/21/77	Complete	Bechtel/SF office	
			C7 06/03/77	Complete	Bechtel/SF office	
CE801	FINEL/FPLOT	Stress analysis for plane or axisymmetric structure	C33 04/15/80	Complete	Bechtel/SF office	3.8.3, 3.8.4
			C32 03/24/80	Complete	Bechtel/SF office	
			C31 08/18/77	Complete	Bechtel/SF office	

TABLE 3A-1 (Cont)

Program			Version Date	Documentation Status		FSAR
No.	Acronym	Description		Verification Report	Location of Verification Document	Reference Section
CE803	ASHSD	Stress analysis for axisymmetric structure under non-axisymmetric loads	C09 02/11/79	Complete	Bechtel/SF office	3.8.3, 3.8.4
			C08 09/27/77	Complete	Bechtel/SF office	
CE901	STRUDL	Design & analysis of beams and frames	1 11/19/80	Complete	Bechtel /SF office	3.8.3, 3.8.4
			F7 06/15/79	Complete	Bechtel/SF office	
			F6 04/02/79	Complete	Bechtel/SF office	
			F5 10/31/77	Complete	Bechtel/SF office	
			F3 11/06/76	Complete	Bechtel/SF office	
CE917	MPS	Modal properties of structures	B5 10/81	Complete	Bechtel/SF office	3.7.2
CE920		Response time history	1 6/20/74	Complete	Bechtel/SF office	3.7.2
CE921		Response spectra	B1 2/15/76	Complete	Bechtel/SF office	3.7.2
CE931		Soil structure interaction	B4 10/81	Complete	Bechtel/SF office	3.7.2
CE991	STARDYNE	General finite element analysis	3 03/03/80	Complete	CDC/SF office	3.8.2, 3.8.3
	BOSOR4	Static stress and stability analysis for axisymmetric and nonaxisymmetric loads	1.0.0 11/27/79	Complete	NUTECH, San Jose	3.8.2
	DECON	Deconvolution analysis	12/5/75	Complete	EDS Nuclear Inc, San Francisco	3.7.2
	EDSGAP	General finite element program	2/20/74	Complete	EDS Nuclear Inc, San Francisco	3.7.2

TABLE 3A-1 (Cont)

Program			Version	Documentation Status		
No.	Acronym	Description	Date	Verification Report	Location of Verification Document	FSAR Reference Section
			3/1/80	Complete	EDS Nuclear Inc, San Francisco	
	FLUSH	Time history response analysis of 2D soil structure	1.0 2/19/83	Complete	UIS/SF office	3.7.2
	RESPEC	Compute response spectra	10/6/75	Complete	EDS Nuclear Inc, San Francisco	3.7.2

APPENDIX 3B

HOPE CREEK GENERATING STATION

UNIT I

MARK I LONG-TERM PROGRAM

PLANT UNIQUE ANALYSIS

FSAR SUMMARY REPORT

Prepared for:

BECHTEL POWER CORPORATION

San Francisco, California

Rev. 0 Prepared by:
NUTECH Engineers, Inc.
San Jose, California

Rev. 1 Prepared by:
Duke Engineering & Services
Naperville, Illinois

TABLE OF CONTENTS

LIST OF TABLES AND FIGURES

I. INTRODUCTION

While in the course of performing large scale testing for Mark III containment systems and in-plant testing for Mark I containment systems, new suppression chamber hydrodynamic loads were identified. The new loads result from a postulated loss-of-coolant accident (LOCA) and safety/relief valve (SRV) operation.

The identification of these new loads presented a generic open item for utilities with Mark I containments. To determine the magnitude, time characteristics, etc, of the dynamic loads in a timely manner, and to identify courses of action needed to resolve any outstanding concerns, these utilities formed the Mark I Owners Group. The Mark I Owners Group established a program which consisted of two parts: 1) A short term program which was completed in 1976, and 2) A long term program which was completed with the submittal of the Mark I Containment Program Load Definition Report (LDR), the Mark I Containment Program Structural Acceptance Criteria Plant Unique Analysis Application Guide (PUAAG) (Reference 4) and supporting reports on experimental and analytical tasks of the Long Term Program (LTP). The NRC reviewed these LTP generic documents and issued acceptance criteria to be used during the implementation of the Mark I plant unique analyses. The NRC acceptance criteria are described in Appendix A of NUREG-0661.

This plant unique analysis (PUA) summary report describes the general approach to be used in the final plant unique analysis report (PUAR) for the HCGS containment. The PUAR will document the detailed evaluation of the modified suppression chamber and internals, which was performed in accordance with the requirements of NUREG-0661.

The purpose of Revision 1 to Appendix B is to address the incorporation of larger suction strainers on the Emergency Core Cooling System (ECCS), Residual Heat Removal (RHR), and Core Spray (CS) penetrations. This is done to address NRC Bulletin 96-03, "Potential Plugging of Emergency Core Cooling Suction Strainers By Debris In Boiling Water Reactors." Note that the PUAR mentioned above will not be revised since it is not maintained as a controlled document.

II. GENERAL DESCRIPTION OF STRUCTURES AND COMPONENTS

Included in this section are brief descriptions of the geometry of the suppression chamber (torus), vent system, torus internal structures and piping, SRV discharge lines, SRV T-quenchers and their supports, and torus-attached piping. Key drawings describing the structural components are also included or referenced.

The Mark I containment is a Pressure Suppression System which houses the boiling water reactor (BWR) pressure vessel, the reactor coolant recirculation loops, and other branch connections of the Nuclear Steam Supply System (NSSS). The containment consists of a drywell, a pressure suppression chamber (wetwell or torus) which is approximately half filled with water, and a vent system which connects the drywell to the wetwell suppression pool. The suppression chamber is toroidal in shape and is located below and encircles the drywell. The drywell to wetwell vents are connected to a vent header contained within the wetwell airspace. Downcomers project downward from the vent header and terminate below the water surface of the suppression pool.

BWR's utilize safety/relief valves attached to the main steam lines as a means of primary system overpressure protection. The outlet of each valve is connected to discharge piping which is routed to the suppression pool. The discharge lines end in T-quencher discharge devices.

Suppression Chamber

Figure 3.8-10 shows the general arrangement of the HCGS suppression chamber. Figure 3.8-11 shows a typical vertical section of the suppression chamber.

Attachments to the suppression chamber include the vent system supports, penetrations, access hatches, supports for the spray header, supports for the monorail and catwalk, supports for the piping, supports for the ECCS (RHR and CS) strainers, and weld pads.

Vent System

The vent system is supported in the suppression chamber by columns, an upper truss, and a downcomer horizontal restraint system. The columns transfer vent system loads to the suppression chamber ring girders. The upper truss connects the vent lines and the vent header to the mitered joint ring girders above. Figures 3.8-15 and 3.8-16 show details of the vent system components and supports.

Torus Internal Structures

The major torus internal structures consist of the catwalk and monorail. Figure 3.8-11 shows their location relative to other components within the suppression chamber. The catwalk is located parallel to the suppression chamber vertical centerline of each mitered cylinder.

SRV Piping

The SRV discharge piping is routed from the SRVs on the main steam line inside the drywell and down the vent lines. The SRV piping exits the vent line and is routed to the nearest mitered joint. It is connected to a T-quencher discharge device. The T-quenchers are supported by a ramshead saddle assembly and the T-quencher arm support beams (Figure II-1).

There are 14 mitered T-quenchers which are centered on the suppression chamber mitered joint ring girders. Each T-quencher consists of a ramshead assembly and two

quencher arms. The ramshead is supported by a saddle and pin plate assembly attached to the ring girder. The T-quenchers have standard General Electric hole pattern designs, but with mitered joints to parallel the quencher arms to the torus axis. The T-quencher arms are supported vertically by support plates attached to T-quencher support beams which span the mitered joint and midcylinder ring beams (Figure II-2). There are 16 support beams to provide a uniform load distribution to the torus.

The T-quencher support system transfers thrust loads and submerged structure loads on the T-quenchers and their supports to the suppression chamber ring girders and shell.

Torus-attached Piping

The torus-attached piping (TAP) consists of 28 major piping systems that are connected to penetrations on the torus shell boundary. The majority of these systems are ECCS related. Fourteen of the systems considered have a segment both external to the torus pressure boundary, and a segment inside the wetwell.

Components included in the PUA evaluations are the piping and piping supports, valves, and branch lines along the pipes. Small Bore Piping Systems, O.D. <4"ϕ, are also included in the evaluation. See Figure II-3 for a graphic representation of a typical TAP system.

III. HYDRODYNAMIC LOADS PHENOMENA

This section presents a summary of the hydrodynamic phenomena and event sequence for postulated LOCA and SRV actuation conditions, which provides the basis for development of the design loading conditions.

LOCA-Related Phenomena

Immediately following a postulated design basis accident (DBA) LOCA, the pressure and temperature of the drywell and vent system atmosphere rapidly increase. With the drywell pressure increase, the water initially present in the downcomers is accelerated into the suppression pool until the downcomers clear of water. Following downcomer water clearing, the downcomer air, which is at essentially drywell pressure, is exposed to the relatively low pressure in the wetwell, producing a downward reaction force on the torus. The consequent bubble expansion causes the pool water to swell in the torus (pool swell), compressing the airspace above the pool. This airspace compression results in an upward reaction force on the torus. Eventually, the bubbles "break through" to the torus airspace, equalizing the pressures. An air/water froth mixture continues upward due to the momentum previously imparted to the water slug, causing impingement loads on elevated structures. The transient associated with this rapid drywell air venting to the pool typically lasts for 3 to 5 seconds.

Following air carryover, there is a period of high steam flow through the vent system. The discharge of steam into the pool and its subsequent condensation causes pool pressure oscillations which are transmitted to submerged structures and the torus shell. This phenomenon is referred to as condensation oscillation (CO). As the reactor vessel depressurizes, the steam flowrate to the vent system decreases. Steam condensation during this period of reduced steam flow is characterized by movement of the water/steam interface up and down within the downcomer as the steam volumes are condensed and replaced by surrounding pool water. This phenomenon is referred to as chugging.

The postulated intermediate break accident (IBA) and small break accident (SBA) produce drywell pressure transients which are sufficiently slow that the dynamic effects of vent clearing and pool swell are negligible. However, CO occurs for an IBA, while chugging occurs for both an IBA and SBA.

SRV Discharge Phenomena

Prior to the initial actuation of an SRV, the safety/relief relief valve discharge lines (SRVDLs) contain air at atmospheric pressure and suppression pool water in the submerged portion of the piping. Following SRV actuation, steam enters the SRVDL, compressing the air within the line and expelling the water slug into the suppression pool. During water clearing, the SRVDL undergoes a transient pressure loading.

Once the water has been cleared from the T-quencher discharge device, the compressed air enters the pool in the form of high pressure bubbles. These bubbles expand, resulting in an outward acceleration of the surrounding pool water. The momentum of the accelerated water results in an overexpansion of the bubbles, causing the bubble pressure to become negative relative to the ambient pressure of the surrounding pool. This negative bubble pressure slows and reverses the motion of the water, leading to a compression of the bubbles and a positive pressure relative to that of the pool. The bubbles continue to oscillate in this manner as they rise to the pool surface. The positive and negative pressures developed due to this phenomenon attenuate with distance and result in an oscillatory pressure loading on the submerged portion of the torus shell and internal structures.

Events Sequence

Not all of the suppression pool hydrodynamic loads occur simultaneously. The load magnitudes and timing also vary, depending on the accident scenario considered. It is therefore necessary to construct a series of event combinations to describe the circumstances under which individual loads might combine. The combinations of load cases were determined from typical plant primary system and containment response analyses.

IV. LOADS AND LOAD COMBINATIONS

This section specifies the categories of SRV and LOCA hydrodynamic loads defined by NUREG-0661 and considered in the HCGS PUA. Loading combinations for each component are also specified. The Primary Containment System is designed for loads resulting from a LOCA and an SRV discharge in accordance with the criteria defined in NUREG-0661 and in the LDR. The loads are developed using the plant unique geometry, operating parameters, and test results contained in the PULD report. Load combinations and fatigue effects are evaluated in accordance with the PUAAG.

Loads

Several loads are included in stress analysis and subsequent evaluations of design margins. For example, the major loads acting on the suppression chamber and on the SRV piping are dead weight, seismic, pressure and temperature, pool swell, condensation oscillation, chugging, and SRV discharge. Vent clearing and vent system and torus interaction loads also act on the SRV piping.

The suppression chamber is subjected to horizontal and vertical accelerations during an operating basis earthquake (OBE) and a safe shutdown earthquake (SSE).

Varying pressure and temperature loads occur during both normal operating conditions and SBA, IBA, or DBA events. The suppression chamber is also subjected to thermal expansion loads associated with normal operating conditions, and other loads associated with these events.

During the initial phase of a DBA event, transient pressures are postulated to act on the suppression chamber shell above and below the suppression pool surface. These loads are based on plant unique Quarter Scale Test Facility (QSTF) test data contained in the PULD and include the effects of the generic spatial distribution factors and of the conservatism factors on the peak upward and downward loads. Pool swell torus shell loads consist of a pseudo static internal pressure component and a dynamic pressure component, and include the effects of the DBA internal pressure. Pool swell loads do not occur during SBA and IBA events.

Transient drag pressures are postulated to act on the submerged suppression chamber components during the air clearing phase of a DBA event. The components affected are the ring girders, vent system supports, submerged piping, and quencher support beams. Harmonic pressures are postulated to act on the submerged portion of the suppression chamber shell during the condensation oscillation phase of DBA and IBA events. In accordance with NUREG-0661, the torus shell loads specified for pre-chug are used in lieu of IBA condensation oscillation torus shell loads. Harmonic drag pressures are postulated to act on the submerged suppression chamber components during the condensation oscillation phase of DBA and IBA events. The components affected are the ring

girders and the quencher support beams. Condensation oscillation loads do not occur during an SBA event.

During the chugging phase of an SBA, IBA, or DBA event, harmonic pressures associated with the pre-chug and post-chug portions of a chug cycle are postulated to act on the submerged portion of the suppression chamber shell. The loading consists of a single harmonic with a specified frequency range and can act either symmetrically or asymmetrically with respect to the vertical centerline of the containment. The symmetric pre-chug load results in vertical loads on the suppression chamber, while the asymmetric pre-chug load results in both vertical and lateral loads on the suppression chamber.

SRV discharge line thrust loads are defined as the pressure and thrust forces acting along the SRV piping due to SRV actuation. The SRV actuation cases considered are: SRV discharge piping thrust loads for normal operating conditions, first actuation; SRV discharge piping thrust loads for normal operating conditions, subsequent actuation; and SRV discharge piping thrust loads for SBA/IBA conditions, first actuation.

SRV T-quencher discharge air clearing loads are defined as the transient pressures that act on the submerged portion of the SRV discharge piping, T-quencher, and their supports during an SRV discharge. These are drag loads acting on the submerged portion of the SRV discharge piping, T-quenchers, and their supports during a DBA event. Acceleration drag loads due to torus fluid-structure interaction (FSI) are included.

Load Combinations

When expanded, the 27 general event combinations given in NUREG-0661 (Tables IV-1 and IV-2) form a large number of load combinations for the Normal Operating, SBA, IBA, and DBA events. The specific load combinations reflect a greater level of detail than is contained in the general event combinations, including distinctions between SBA and IBA, beween pre-chug and post-chug, between SRV actuation cases, and consideration of multiple cases of particular loadings. Several different service level limits and corresponding sets of allowable stresses are associated with these load combinations.

Not all of the possible load combinations are evaluated since many are enveloped by other combinations and do not lead to controlling stresses. The enveloping load combinations are determined by examining all possible load combinations and by comparing the respective load cases and allowable stresses.

The enveloping load combinations are reduced further by examining relative load magnitudes and individual load characteristics to determine which load combinations lead to controlling stresses.

V. ACCEPTANCE CRITERIA

This section explains the criteria used in the LDR and NUREG-0661, including any exceptions or interpretations.

The acceptance criteria used in the PUA have been developed from the NRC review of the LTP, LDR, the PUAAG, and the supporting analytical and experimental programs conducted by the Mark I Owners Group. These criteria are documented in NUREG-0661 for both hydrodynamic load definitions and structural applications.

Hydrodynamic Loads: NRC Acceptance Criteria

Appendix A of NUREG-0661 resulted from the NRC evaluation of the load definition procedures for suppression pool hydrodynamic loads, which were proposed by the Mark I Owners Group for use in their plant unique analyses. This NRC evaluation addressed only those events or event combinations that involve suppression pool hydrodynamic loads. The NRC hydrodynamic loads acceptance criteria are used with a coupled fluid structure analytical model.

Where feasible, the NUREG-0661 acceptance criteria were used in the detailed plant unique load determinations and associated structural analyses. Where this simple, direct approach resulted in unrealistic hydrodynamic loads, more sophisticated plant unique analyses were performed. Many of these analyses have indicated that a specific interpretation of the generic rules was quite reasonable. These specific interpretations of the generic hydrodynamic acceptance criteria are identified as follows.

The hydrodynamic loads criteria are based on NRC review of and revision to experimentally formulated hydrodynamic loads. Pool swell loads derived from plant unique quarter scale two dimensional tests are used to obtain net torus up and down loads and local pressure distributions. Vent system impact and drag loads resulting from pool swell effects are also based on experimental results, using analytical techniques where appropriate.

Condensation oscillation and chugging loads were derived from Full Scale Test Facility (FSTF) results. Condensation oscillation and post-chug torus shell and

submerged structure loads are defined in terms of 50 harmonics. Random phasing of the loading harmonics is assumed, based on FSTF data and subsequent analysis.

NUREG-0661 states that the FSI effect on condensation oscillation and on chugging submerged structure loads can be accounted for by adding the shell boundary accelerations to the local fluid acceleration. The FSI effect for a given structure is included by adding the pool fluid acceleration at the location of the structure, rather than the shell boundary acceleration.

The analysis techniques for SRV loads were developed to generically define T-quencher air clearing loads on the torus. However, a number of Mark I licensees have indicated that the generic load definition procedures are overly conservative for their plant design, especially when the procedures are coupled with conservative structural analysis techniques. To allow for these special cases, the NRC has stipulated requirements whereby in-plant tests could be used to derive the plant specific structural response to the SRV air clearing loads on the torus.

Because of the various phenomena associated with the air clearing phase of SRV discharge, some form of analysis procedure is necessary to extrapolate from test conditions to the design cases. Therefore, the NRC requirements are predicated on formulating a coupled load structure analysis technique which is calibrated to the plant specific conditions for the simplest form of discharge (i.e., single valve, first actuation) and then applied to the design basis event conditions.

SRV torus shell loads are evaluated using the alternate approach of NUREG-0661, which allows the use of inplant SRV tests to calibrate a coupled load-structure

analytical model. This method utilizes shell pressure waveforms more characteristic of those observed in tests. For SRV bubble induced drag loads on submerged structures, a bubble pressure multiplier is used that bounds the maximum peak positive bubble pressure and the maximum bubble pressure differential observed during the Monticello T-quencher tests. A series of inplant SRV tests will be performed after fuel load to confirm that the computed loadings and predicted structural responses for SRV discharges are conservative.

Several loads are classified as secondary loads because of their inherent low magnitudes. These loads include seismic slosh pressure loads, post-pool swell wave loads, asymmetric pool swell pressure loads, sonic and compression wave loads, and downcomer air clearing loads. These secondary loads are treated as negligible compared to other loads in the PUA, which is in accordance with Appendix A of NUREG-0661.

Service Level Assignments

The service level criteria used in the HCGS plant unique analysis to evaluate the acceptability of the containment design, or to provide the basis for any plant modifications, are in accordance with Section III of the ASME Boiler and Pressure Vessel Code through the Summer 1977 Addenda (Reference 5).

Service Limits

The service limits are defined in terms of the Winter 1976 Addenda, which introduced Levels A, B, C, and D. The selection of specific service limits for each load combination is dependent on the functional requirements of the component analyzed and the nature of the applied load. The structures and components in the containment

system are categorized in accordance with their functions in order to assign the appropriate service limits. The general components of the HCGS containment have been classified in accordance with the American Society of Mechanical Engineers (ASME) Boiler and Pressure Vessel Code as specified in NUREG-0661.

Table V-I provides a listing of the applicable ASME Code Addenda, Subsection, and Service Level as appropriate for the criteria/components included in the plant unique analysis.

VI. ANALYTICAL PROCEDURES

The methods of analysis and computer programs used for all the structures and components under evaluation are explained with a brief description of the mathematical models and assumptions used. Deviations from the standard methods or computer programs established in the industry are identified.

Descriptions of the computer models used in the suppression chamber analysis and the analytical techniques used in the suppression chamber penetration analysis are provided in the following paragraphs.

1/32 Segment Torus Finite Element Model

Figure 3.8-20 shows a typical 1/32 segment finite element model. Additional mesh refinement is included in modeling the column connections, the horizontal restraints, and the adjacent torus shell. The model includes the midcylinder ring girder and the miter joint ring girder.

The model is used to evaluate the effects of normal and hydrodynamic loads and reactions taken from the analyses of the vent system, internal structures, and internal

piping. The model is also used to generate torus shell motions for use in the torus attached piping analysis. Stresses in the torus shell, ring girders, columns and column connections, horizontal restraint beams and pad plate, and associated welds are calculated using results from this model.

Static analyses of the model are performed for normal loads and applicable reaction loads taken from the analysis of the above mentioned structures. A dynamic analysis of the model is performed for hydrodynamic loads using the modal superposition technique. Fluid structure interaction is addressed through the use of a fluid added mass formulation.

1/32 Segment Vent System Finite Element Model

A finite element model of a 1/32 segment of the vent system (Figure VI-1) is used to evaluate the local effects of pool swell impact. The model extends from the miter joint to midcylinder of the non-vent bay. The model includes the vent header, the downcomers, the downcomer stiffening and bracing, the miter joint and midcylinder support rings, the lower columns, and the upper truss. A beam representative of the vent system in the vent bay is included to account for the overall response of the vent system. A dynamic analysis of the model is performed using the modal superposition technique.

The maximum stresses computed for the vent header, downcomers, and downcomer stiffening plates are added to those computed for other loadings in the intersection model analyses. (Analysis shows the vent header is adequate without a deflector.)

1/16 Segment Vent System Beam Model

The beam model of a 1/16 segment of the vent system is similar to that shown in Figure 3.8-21. The model includes the vent line, vent header, downcomers, down-comer bracing, vacuum breaker support, upper truss, lower columns, T-quenchers, and T-quencher supports. Stiffnesses for modeling of vent system-torus shell intersection are obtained from unit load analyses of finite element models. The coupling effects of the suppression chamber are modeled by including a coarse grid representation of the torus shell and the ring girders and torus supports. The model also includes the SRV piping and its supports inside the suppression chamber up to the vent line penetration.

The model is used to evaluate the effects of normal and hydrodynamic loads. Stresses in the vent system supports, downcomer bracing, and SRV piping are calculated using results from this model. In addition, the model is used to generate boundary loads, support loads, and distributed loads for use in the intersection model analyses.

Static analyses of the model are performed for normal loads. A dynamic analysis of the model is performed for hydrodynamic loads and SRV piping thrust loads using the modal superposition technique.

Downcomer Vent Header Intersection Model

The finite element model of a typical downcomer vent header intersection is similar to that shown in Figure 3.8-24. The model includes a portion of the vent header and downcomers and the intersection stiffening plates, such as the crotch plate, downcomer rings, and outer gusset plates. The model is used to evaluate the

effects of boundary loads, support loads, and distributed loads taken from the 1/16 segment beam model. Stresses in the vent header, downcomers, intersection stiffening plates, and associated welds are calculated using results from this model.

Vent Line Vent Header Intersection Model

The finite element model of a vent line vent header intersection is similar to that shown in Figure 3.8-23. The model includes a portion of the vent line and vent header, the vent line end plate, and the vacuum breaker

support. The model is used to evaluate the effects of boundary loads, support loads, and distributed loads taken from the 1/16 segment beam model. Stresses in the vent line, vent header, vent line end plate, vacuum breaker support, and associated welds are calculated using results from this model.

Vent Line-Drywell Intersection Model

The finite difference model of a vent line drywell intersection is similar to that shown in Figure VI-2. The model includes a portion of the drywell shell and vent line, the insert plate, the conical transition, and the jet deflector. The model is used to evaluate the effects of the beam loads taken from the 1/16 segment beam model analysis. Stresses in the drywell shell, vent line, insert plate, and conical transition are calculated using results from this model.

Suppression Chamber Internal Structures and Supports

The suppression chamber monorail and the suppression chamber walkways and ladders are analyzed for normal, seismic, and hydrodynamic loads using beam type computer

models and/or manual calculations. The support reactions at the torus ring girders computed in these analyses are applied to the suppression chamber 1/32 segment finite element model.

SRV Piping and Supports

The SRV piping inside the suppression chamber is analyzed for loads directly applied to the piping analytical model, as well as for loads derived from the 1/16 segment beam model vent system analysis. Nodal loads taken from the results of the governing load combinations are applied to separate internal piping models. Stresses are calculated and an ASME Code evaluation performed using the PISTAR piping analysis program; see Reference 6. Stresses for internal piping supports and associated welds are computed for the governing load combinations using hand calculation methods.

The SRV piping systems are modeled as multiple degree of freedom, finite element systems consisting of straight and curved beam elements using a lumped mass formulation. A sufficient amount of detail is used to accurately represent the dynamic behavior of the piping systems for the applied loads. Flexibility and stress intensification factors based on the ASME Code, Section III, Class 2 piping requirements are also included in the model formulations. A typical wetwell SRV piping system is modeled from the vent pipe penetration down to and including the T-quencher; see Figure II-1.

The T-quencher and T-quencher supports are evaluated for the effects of loads using the vent system 1/16 segment beam model. The analytical model includes the SRV line in the wetwell from the vent line/SRV piping penetration to the ramshead, the ramshead assembly, the quencher arms,

the quencher support beam, and the associated connecting and support members.

The PISTAR piping model is used to perform dynamic analyses for the SRV discharge and seismic loads acting on the SRV piping. A time history analysis is performed for the SRV discharge transient thrust forces acting along the SRV piping. A response spectrum analysis is performed for both OBE and SSE loadings.

The remaining load cases affecting the SRV piping are evaluated using the vent system 1/16 segment beam model. These load cases consist of hydrodynamic loads analyzed using dynamic or equivalent static techniques and remaining normal and Mark I interaction loads.

The analysis procedure used in performing the fatigue evaluation for SRV wetwell piping is based on a formulation similar to Equation 11 of the ASME Code, Section III, Subsection NC. The fatigue evaluation involves determining the allowable number of stress cycles for each load combination using Markl's fatigue equation. The calculation of fatigue usage factors for each loading combination is performed by dividing the effective number of maximum stress cycles by the allowable number of stress cycles. The summation of usage factors for all the potential load combinations that can occur during the plant life results in the maximum cumulative usage factor.

Torus Attached Piping

The analysis and evaluation of the torus attached piping (TAP) use the Nutech proprietary piping analysis program PISTAR, noted in Reference 6. The piping systems are modeled from the torus to their first external anchor points. Piping inside the torus is also included in the

models. Large branch lines, i.e., where the ratio of run pipe to branch pipe diameter is less than three, are included in the models. Small diameter torus attached and branch piping (<4 inch diameter) is evaluated separately, using either dynamic or equivalent static analytical techniques.

TAP is analyzed for torus motions resulting from hydrodynamic loadings. The torus motions are obtained from the torus analysis. Torus internal portions of the piping are analyzed for the effects of directly applied hydrodynamic loadings using dynamic and equivalent static techniques. The piping is also analyzed for normal operating conditions, i.e., pressure, dead weight, and temperature, and seismic loadings. The methods of analysis used for these loadings are consistent with the methods used in the original analysis.

An evaluation of the acceptability of the TAP is performed in compliance with the Class 2 and 3 design rules of the ASME Code, Section III, the PUAAG, and the HCGS design specification. These evaluations include load combinations, design limits, stress intensification factors (SIF), allowable valve accelerations, flange evaluations, and equipment nozzle loads.

The analysis procedure used in performing the fatigue evaluation for the TAP is the same as described for the SRV piping.

VII. STRUCTURAL EVALUATION

The structural evaluation summary includes the results of the analysis and a description of structure or component modifications. Specific evaluations for various portions of the analysis are given in the following paragraphs.

Membrane and extreme fiber stress intensities are computed when the analysis results for the suppression chamber Class MC components are evaluated. The values of the membrane stress intensities away from discontinuities are compared with the primary membrane stress allowables. The values of membrane stress intensities near discontinuities are compared with local primary membrane stress allowables. Primary stresses in suppression chamber Class MC component welds are computed using the maximum principal stress or resultant force acting on the associated weld throat. The results are compared to the primary weld stress allowables.

Many of the loads contained in each of the controlling load combinations are dynamic loads resulting in stresses that cycle with time and are partially or fully reversible. The maximum stress intensity range for all suppression chamber Class MC components is calculated using the maximum values of the extreme fiber stress differences which occur near discontinuities. These values are compared with secondary stress range allowables. A similar procedure is used to compute the stress range for the suppression chamber Class MC component welds. The results are compared to the secondary weld stress allowables.

During load combination formulation, the maximum stress components in a particular suppression chamber component at a given location are combined for the individual loads contained in each combination. The stress components for dynamic loads are combined to obtain the maximum stress intensity.

For evaluating fatigue effects in the suppression chamber Class MC components and associated welds, extreme fiber alternating stress intensity histrograms for each load in each event or combination of events are determined.

Stress intensity histograms are developed for the suppression chamber components and welds with the highest stress intensity ranges. Fatigue strength reduction factors of 2.0 for major component stresses and 4.0 for component weld stresses are conservatively used. For each combination of events, a load combination stress intensity histrogram is formulated and the corresponding fatigue usage factors are determined. The usage factors for each event are than summed to obtain the total fatigue usage.

A bounding analysis was developed to identify the need for torus modifications on a schedule compatible with plant construction. Any modifications to the torus structure would be identified on the basis of the best available information and limited design analysis, with final design verification obtained from detailed stress analysis as part of the PUAR. Upper bound estimates of the total integrated load expected in the PUA were determined.

The estimated total integrated load per mitered cylinder is 4600 kips upward and 5600 kips downward, with the estimated primary membrane stress capacity of the torus shell at the 7400 kips per mitered cylinder. The estimated capacities of column supports are 5000 kips upward and 6500 kips downward per mitered cylinder.

Analytical results show that minor modifications are appropriate for the torus shell at the top of the column pin plates, at the ring girder/column connections, and for the ring girder and torus shell at the tips of the midcylinder ring girders and column base plates. Figure VII-1 shows extended column connection pin plates, flange plates, ring girder cover plates, midspan ring stiffeners and baseplate stiffeners.

The results of the structural evaluation of the torus indicate that the largest suppression chamber shell stresses occur for IBA internal pressure loads, pool swell torus shell loads, DBA condensation oscillation torus shell loads, and SRV discharge torus shell loads. In general, the submerged structure loadings cause only local stresses in the suppression chamber shell adjacent to the vertical quencher support beam and the ring girder.

The largest suppression chamber vertical support reactions occur for pool swell torus shell loads, DBA condensation oscillation loads, and SRV discharge torus shell loads.

The largest stresses in the suppression chamber components, component supports, and associated welds occur for the IBA load combinations. The suppression chamber shell stresses for the IBA combinations are less than the allowable limits, with stresses in the suppression chamber components, component supports, and welds well within the allowable limits. The stresses in the suppression chamber components, component supports, and welds for the DBA combinations are also well within the allowable limits.

The largest upward and downward vertical support reactions occur for the SBA and IBA combinations. In general, the upward vertical support reactions are less than the downward vertical support reactions. The vertical support system reactions for all load combinations are less than the allowable limits.

The largest seismic restraint reactions and associated suppression chamber shell stresses occur for seismic loads and SRV discharge loads. The seismic restraint reactions and suppression chamber shell stresses adjacent to the seismic restraints for IBA load combinations are less than the allowable limits.

The largest contributor to the suppression chamber fatigue effects are SRV discharge loads that occur during normal operating conditions. The largest total fatigue usage occurs for the Normal Operating plus SBA events, with usage factors for the suppression chamber shell and associated welds less than the allowable limits. The usage factors for the Normal Operating plus IBA events are also less than the allowable limits.

The largest vent system stresses occurred for DBA pool swell impact combined with internal pressure (Service Level B) and for pool swell impact combined with SRV downcomer drag and internal pressure (Service Level C). Stresses for both limiting loading combinations were considerably less than the allowables, with the maximum stress intensity in the vent header occurring at the vent header-downcomer intersection (at 57 percent of the allowable and with downcomer stresses at 43 percent of the allowable), and very small stresses in miscellaneous support plates. Although additional, somewhat less significant loadings for dead weight, seismic, thermal expansion and submerged structures effects are included in the final PUAR, margins are of sufficient magnitude in the current analysis to allow the decision to be made to not require vent header deflectors.

The results indicate that the largest vent system primary membrane stresses occur for internal pressure loads, vent system discharge loads, pool swell impact loads, DBA condensation oscillation downcomer loads, and chugging downcomer lateral loads. The remaining loads result in small primary stresses in the vent system major components.

The largest vent system support column reactions occur for internal pressure loads, vent system discharge loads, pool swell impact loads, and DBA condensation oscillation

loads. The distribution of loads between the inner and outer support columns varies from load case to load case. The magnitude and distribution of reaction loads on the drywell penetrations also vary from load case to load case.

The highest stresses in the vent system components, component supports, and associated welds occur for the SBA and the DBA load combinations. The vent line, vent header, and downcomer stresses for the SBA and DBA load combination are less than the allowable limits, with stresses in other vent system components, component supports, and welds well within the allowable limits.

The stresses in the vent system components, component supports, and welds for the IBA and DBA load combinations are also well within the allowable limits.

The vent system fatigue usage factors are computed for the controlling events, which are Normal Operating plus SBA and Normal Operating plus IBA. The governing vent system component for fatigue is the vent header at the downcomer vent header intersection. The magnitudes and cycles of downcomer lateral loads are the primary contributors to fatigue at this location.

The governing vent system weld for fatigue is the nozzle to gusset weld at the SRV vent line penetration. SRV temperature and thrust loads and the number of SRV actuations are the major contributors to fatigue at this location.

Fatigue effects at other locations in the vent system are less severe than at those described above, primarily due to lower stresses and a lesser number of stress cycles.

The maximum resultant stresses in the SRV wetwell piping supports on the vent line and vent header for each service level (along with the associated allowable stress values) show that the design of the SRV piping system is adequate for the loads, load combinations, and acceptance criteria limits specified in NUREG-0661 and in the PUAAG.

Analysis of large bore torus attached piping systems indicates that piping and its supports meet acceptance criteria. Some torus attached small bore piping and small bore piping attached to larger systems have been modified to meet acceptance criteria.

VIII. SUMMARY AND CONCLUSIONS

A summary of the structures evaluated, the loadings considered, the modifications, and a final concluding statement referring to the margins of safety is presented.

The loads considered in the original design of the primary containment system include dead weight loads, OBE and SSE loads, and pressure and temperature loads associated with normal operating conditions (NOC) and a postulated LOCA event. Additional loadings postulated to occur during SBA, IBA, or DBA LOCA events, and during SRV discharge events that affect the design of the primary containment system, are defined generically in NUREG-0661. Each of these events results in hydrodynamic pressure loadings on the primary containment system shell, hydrodynamic drag loadings on the submerged components of the primary containment system, and in reaction loadings caused by loads acting on structures attached to the primary containment system.

The methodology used to develop plant unique loadings for the primary containment system evaluation results in conservative values for each of the significant

NUREG-0661 loadings which envelop those postulated to occur during an actual LOCA or SRV discharge event.

The LOCA related and SRV discharge related loads are grouped into event combinations using NUREG-0661 criteria. The event sequencing and event combinations specified and evaluated envelop the actual events expected to occur throughout the life of the plant. Some of the loads contained in the postulated event combinations are major contributors to the total response of the primary containment system. These include LOCA internal pressure loads, DBA pool swell torus shell loads, DBA condensation oscillation torus shell loads, and SRV discharge torus shell loads. Although considered in the evaluation, other loadings such as temperature loads, seismic loads, chugging torus shell loads, submerged structure loads, and containment structure reaction loads, have a lesser effect on the total response of the primary containment system.

The Primary Containment System evaluation is based on NUREG-0661 structural acceptance criteria. These acceptance limits are at least as restrictive as those used in the original primary containment system design. Use of this criteria ensures that the original primary containment system design margins have been restored.

The controlling event combinations for the primary containment system include the loadings which have been found to be major contributors to the primary containment system response. The evaluation results for these controlling event combinations show that all of the primary containment system stresses and support reactions are within acceptable limits.

As a result, the Primary Containment System has margins of safety inherent in its original design. The NUREG-0661

requirements as they affect the design adequacy and safe operation of the HCGS primary containment system are met.

Detailed justification of the plant unique containment analysis has been submitted under separate cover (letter from R.L. Mittl, PSE&G, to A. Schwencer, NRC, dated February 10, 1984) in the form of a HCGS Plant Unique Analysis Report.

IX. REFERENCES

1. "Mark I Containment Program Load Definition Report," General Electric Company, NEDO-21888, Revision 2, December 1981.

2. "Mark I Containment Program Plant Unique Load Definition," HCGS Generating Station Unit 1, General Electric Company, NEDO-24579, Revision 1, January 1982.

3. "Mark I Containment Long Term Program," Safety Evaluation Report, USNRC, NUREG-0661, July 1980; Supplement 1, August 1982.

4. "Mark I Containment Program Structural Acceptance Criteria Plant Unique Analysis Applications Guide," Task Number 3.1.3, Mark I Owners Group, General Electric Company, NEDO-24583, Revision 1, July 1979.

5. ASME Boiler and Pressure Vessel Code, Section III Division 1, 1974 Edition with Addenda up to and including Summer 1977.

6. Nuclear Technology, Inc., "PISTAR User;s Manual," NUTECH Topical Report Number TR-76-002, Revision 2, September 1979.

APPENDIX 3B

TABLE IV-1

MARK I CONTAINMENT EVENT COMBINATIONS
FOR CLASS MC COMPONENTS & INTERNAL STRUCTURES
(FROM NUREG-0661)

Event Combinations	SRV	EQ	SRV +			SBA IBA		SBA + EQ IBA + EQ					SBA+SRV IBA+SRV		SBA + SRV + EQ IBA + SRV + EQ				DBA		DBA + EQ						DBA+SRV		DBA + SRV + EQ			
							CO, CN					CO,CN				CO,			CO,CN			PS	CN	CO, PS			CO,CN		PS	CN	CO, PS			CO,CN
Type of Earthquake				O	S				O	S	O	S				O	S	O	S						O	S	O	S				O	S	O	S
Combination Number		1	2	3	4	5	6	7	8	9	10	11	12	13	14	15	16	17	18	19	20	21	22	23	24	25	26	27						
Loads																																		
Normal(2)	N	X	X	X	X	X	X	X	X	X	X	X	X	X	X	X	X	X	X	X	X	X	X	X	X	X	X	X						
Earthquake	EQ		X	X			X	X	X	X			X	X	X	X			X	X	X	X			X	X	X	X						
SRV discharge	SRV	X	X	X							X	X	X	X	X	X							X	X	X	X	X	X						
LOCA thermal	T_A				X	X	X	X	X	X	X	X	X	X	X	X	X	X	X	X	X	X	X	X	X	X	X	X						
LOCA reactions	R_A				X	X	X	X	X	X	X	X	X	X	X	X	X	X	X	X	X	X	X	X	X	X	X	X						
LOCA quasi-static pressure	P_A				X	X	X	X	X	X	X	X	X	X	X	X	X	X	X	X	X	X	X	X	X	X	X	X						
LOCA pool swell	P_{PS}																X		X	X			X		X	X								
LOCA condensation oscillations	P_{CO}					X			X	X		X			X	X		X			X	X		X			X	X						
LOCA chugging	P_{CN}					X			X	X		X			X	X		X			X	X		X			X	X						
Structural Element	Row																																	
External Class MC																																		
Torus, external vent pipe, bellows, drywell (at vent), attachment welds, torus supports, seismic restraints	1	A	B	C	A	A	B	C	B	C	A	A	B	C	B	C	A (3, 6)	A	B (3, 6)	C	B	C	C	C	C	C	C	C						

TABLE IV-1 (Cont)

Event Combinations		SRV	SRV + EQ	SBA IBA	SBA + EQ IBA + EQ					SBA+SRV IBA+SRV			SBA + SRV + EQ IBA + SRV + EQ			DBA		DBA + EQ				DBA+SRV		DBA + SRV + EQ			
				CO, CN						CO, CN							PS	CO, PS						CO, PS			
Type of Earthquake			O	S			O	S	O	S			O	S	O	S			O	S	O	S			O	S	O	S
Combination Number																												
Loads	1	2	3	4	5	6	7	8	9	10	11	12	13	14	15	16	17	18	19	20	21	22	23	24	25	26	27	
Internal Vent Pipe																												
General and attachment welds	2	A	B	C	A	A	B	C	B	C	A	A	B	C	B	C	A (3, 5)	A	B (3, 5)	C	B	C	C	C	C	C	C	C
At penetrations (e.g., header)	3	A	B	C	A	A	B	C	B	C	A	A	B	C	B	C	A (3)	A	B (3)	C	B	C	C	C	C	C	C	C
Vent Header																												
General and attachment welds	4	A	B	C	A	A	B	C	B	C	A	A	B	C	B	C	A (3, 5)	A	B (3, 5)	C	B	C	C	C	C	C	C	C
At penetrations (e.g., downcomers)	5	A	B	C	A	A (4)	B	C	B (4)	C	A	A (4)	B	C	B (4)	C	A (3, 4,5)	A (4)	B (3, 4,5)	C	B (4)	C	C	C	C	C	C	C
Downcomers																												
General and attachment welds	6	A	B	C	A	A	B	C	B	C	A	A	B	C	B	C	A (3, 5)	A	B (3, 5)	C	B	C	C	C	C	C	C	C
Internal Supports	7	A	B	C	A	A	B	C	B	C	A	A	B	C	B	C	A	A	B	C	B	C	C	C	C	C	C	C
Internal Structures																												
General	8	A	B	C	A	A	C	D	C	D	C	C	D	E	D	E	E	E	E	E	E	E	E	E	E	E	E	E
Vent deflector	9	A	B	C	A	A	C	D	C	D	C	C	D	D	D	D	D	D	D	D	D	D	D	D	D	D	D	D

APPENDIX 3B

TABLE IV-2

MARK I CONTAINMENT EVENT COMBINATIONS
AND SERVICE LEVELS FOR CLASS 2 AND 3 PIPING
(FROM NUREG-0661)

Event Combinations		SRV	SRV + EQ		SBA	SBA IBA CO, CN		SBA + EQ IBA + EQ CO,CN			SBA+SRV	SBA + SRV + EQ IBA+SRV CO, CN			IBA + SRV + EQ CO,CN		PS (1)	DBA CO, CN	PS		DBA + EQ CO, CN		PS	DBA+SRV CO, CN	PS		DBA + SRV + EQ CO, CN	
Type of Earthquake			O	S			O	S	O	S			O	S	O	S				O	S	O	S			O	S	O	S
Combination Number		1	2	3	4	5	6	7	8	9	10	11	12	13	14	15	16	17	18	19	20	21	22	23	24	25	26	27
Loads																												
Normal(2)	N	X	X	X	X	X	X	X	X	X	X	X	X	X	X	X	X	X	X	X	X	X	X	X	X	X	X	X
Earthquake	EQ		X	X			X	X	X	X			X	X	X	X			X	X	X	X			X	X	X	X
SRV discharge	SRV	X	X	X							X	X	X	X	X	X							X	X	X	X	X	X
Thermal	T	X	X	X	X	X	X	X	X	X	X	X	X	X	X	X	X	X	X	X	X	X	X	X	X	X	X	X
Pipe pressure	P	X	X	X	X	X	X	X	X	X	X	X	X	X	X	X	X	X	X	X	X	X	X	X	X	X	X	X
LOCA pool swell	P																X		X	X			X		X	X		
LOCA condensation oscillations	P					X			X	X		X			X	X		X			X			X			X	
LOCA chugging	P					X			X	X		X			X	X		X			X	X		X			X	X
Structural Element	Row																											
Essential Piping Systems																												
With IBA/DBA	10	B	B (3)	B (3)	B (4)	B (4)	B (4)	B (4)	B (4)	B (4)	B (4)	B (4)	B (4)	B (4)	B (4)	B (4)	B (4)	B (4)	B (4)	B (4)	B (4)	B (4)	B (4)	B (4)	B (4)	B (4)	B (4)	B (4)
With SBA	11				B (3)	B (3)	B (4)	B (4)	B (4)	B (4)	B (3)	B (3)	B (4)	B (4)	B (4)	B (4)	-	-	-	-	-	-	-	-	-	-	-	-

TABLE IV-2 (Cont.)

Event Combinations		SRV	SRV + EQ		SBA	SBA + EQ					SBA+SRV	SBA + SRV + EQ						DBA			DBA + EQ				DBA+SRV		DBA + SRV + EQ		
					IBA			IBA + EQ			IBA+SRV	IBA + SRV + EQ					PS	DBA			DBA + EQ				DBA+SRV		DBA + SRV + EQ		
					CO, CN				CO,CN		CO, CN			CO,CN			(1)	CO, CN		PS		CO,	CN	PS	CO, CN			CO,	CN
Type of Earthquake			O	S		O	S	O	S			O	S	O	S					O	S	O	S			O	S	O	S
Combination Number		1	2	3	4	5	6	7	8	9	10	11	12	13	14	15	16	17	18	19	20	21	22	23	24	25	26	27	
Loads																													
Nonessential Piping Systems																													
With IBA/DBA	12	B	C (5)	D (5)	D (5)	D (5)	D (5)	D (5)	D (5)	D (5)	D (5)	D (5)	D (5)	D (5)	D (5)	D (5)	D (5)	D (5)	D (5)	D (5)	D (5)	D (5)	D (5)	D (5)	D (5)	D (5)	D (5)	D (5)	D (5)
With SBA	13				C (5)	C (5)	D (5)	D (5)	D (5)	D (5)	D (5)	D (5)	D (5)	D (5)	D (5)	D (5)	-	-	-	-	-	-	-	-	-	-	-	-	-

APPENDIX 3B

TABLE V-1

ASME CODE APPLICABILITY[1]

Criteria/ Component[2]	Addenda	Code Subsection
Service Levels A through D	Summer 1977	N/A
Service Limits	Winter 1976	N/A
Structural Acceptance Criteria	Summer 1977	NE for Class MC components
Suppression chamber shell and ring girder	Summer 1977	NE for Class MC components
Fillet welds and partial penetration welds	Summer 1977	NE for Class MC component attach-welds
Suppression chamber columns, column connections, and associated component parts and welds	Summer 1977	NF for Class MC component supports
Quencher support beam	Summer 1977	NF for Class 3 component supports
Vent lines, vent header, downcomers, support column ring plate, drywell shell, downcomer-vent header intersection stiffener plates, vent line-vent header intersection, vacuum breaker nozzle, vent line-SRV piping penetration assembly	Summer 1977	NE for Class MC components

TABLE V-1 (Cont.)

Criteria/ Component[2]	Addenda	Code Subsection
Support columns, downcomer bracing members	Summer 1977	NF for Class MC component supports
Internal structures	Summer 1977	NF for Class MC component supports[3]
SRV piping	Summer 1977	ND for Class 3 piping
SRV piping supports	Summer 1977	NF for Class 3 piping supports
T-quencher arms	Summer 1977	ND for Class 3 piping
Ramshead	Summer 1977	ND for Class 3 piping
T-quencher and ramshead supports	Summer 1977	NF for Class 3 piping supports
Torus attached piping (TAP)	Summer 1977	NC for Class 2 piping
		ND for Class 3 piping
TAP supports	Summer 1977	NF for Class 3 supports

TABLE V-1 (Cont)

---

(1) Section III, Division 1.

(2)

	Maximum Temp.
Suppression chamber	167°F
Vertical support system	100°F
Column base plate	100°F
Vent system	212°F

(3) With Service Level D allowable limits.

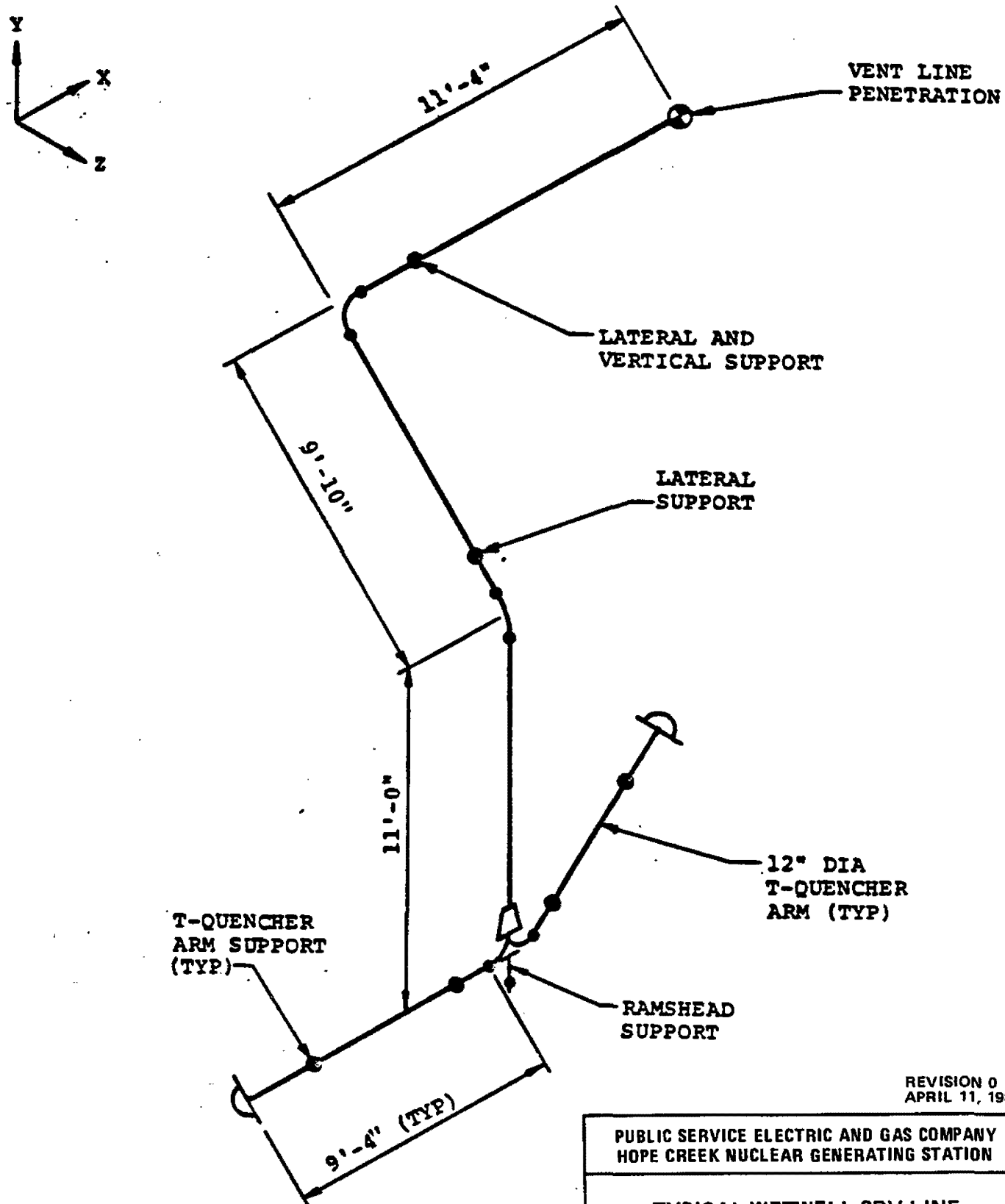

REVISION 0
APRIL 11, 1988

PUBLIC SERVICE ELECTRIC AND GAS COMPANY
HOPE CREEK NUCLEAR GENERATING STATION

TYPICAL WETWELL SRV LINE
ISOMETRIC AND SUPPORT LOCATIONS

UPDATED FSAR

Appendix 3B
FIGURE II-1

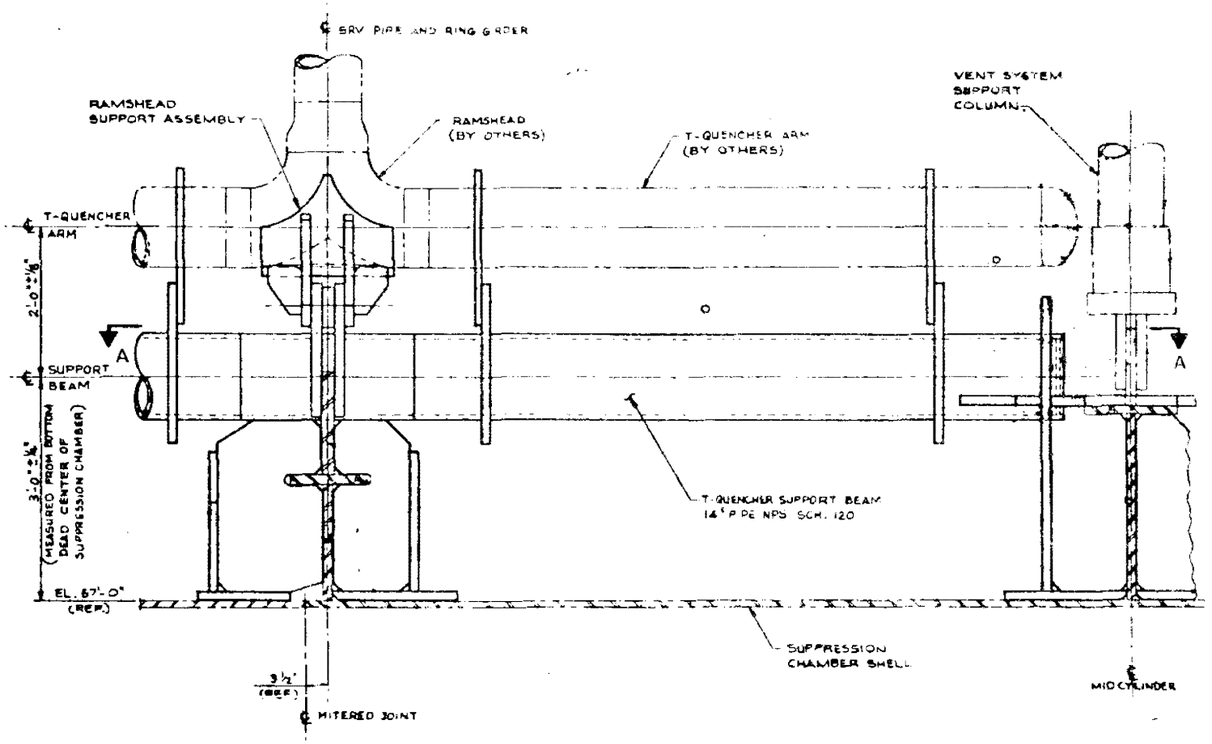

ELEVATION VIEW

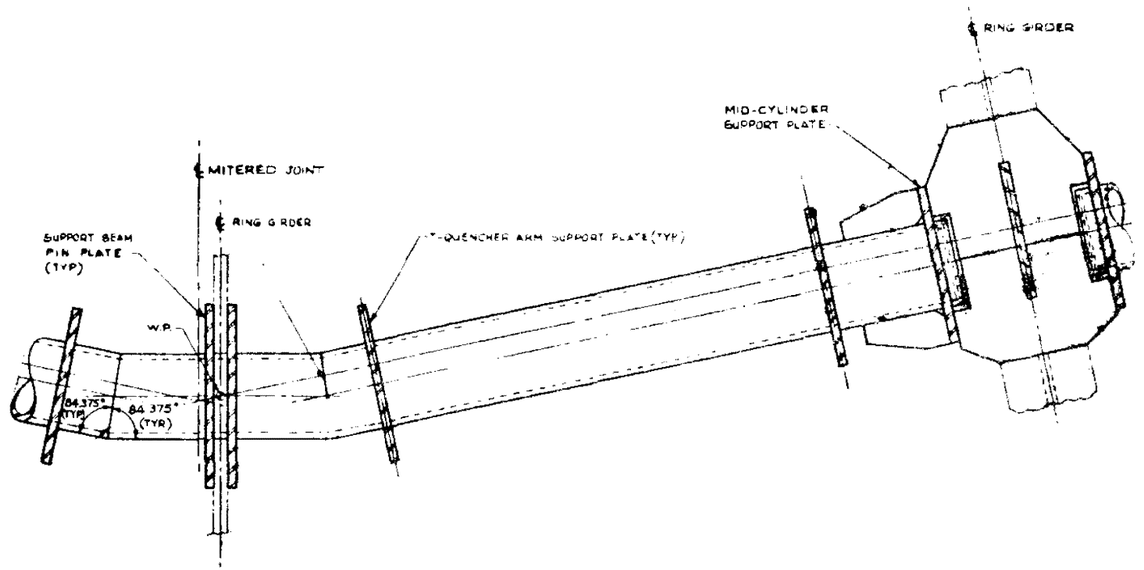

SECTION A–A

REVISION 0
APRIL 11, 1988

PUBLIC SERVICE ELECTRIC AND GAS COMPANY
HOPE CREEK NUCLEAR GENERATING STATION

ELEVATION AND SECTION VIEWS OF T – QUENCHER SUPPORT DETAILS

UPDATED FSAR

Appendix 3B
FIGURE II-2

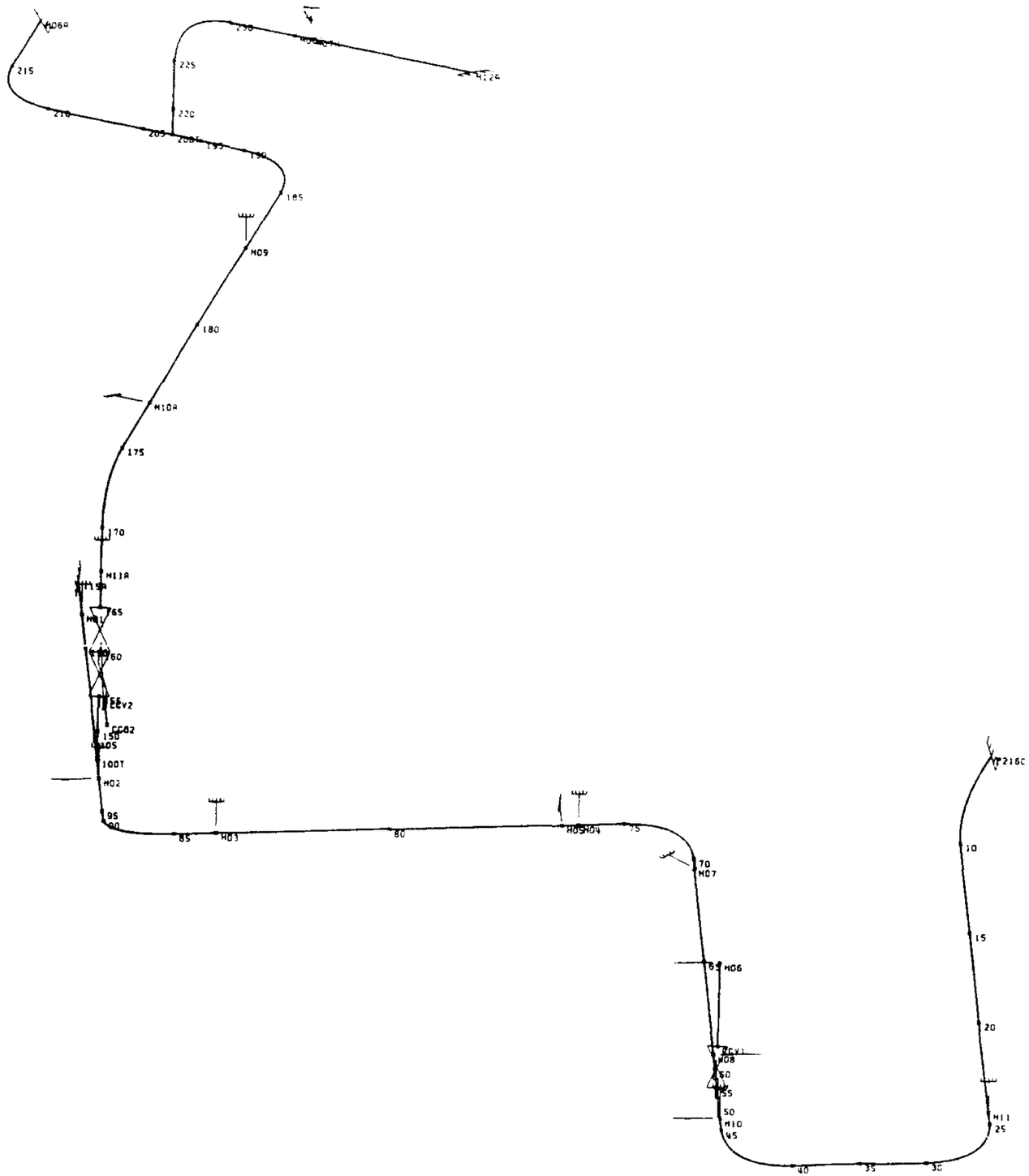

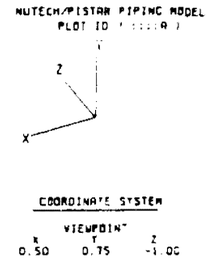

CORE SPRAY PUMP SECTION(C)-P216C

REVISION 0
APRIL 11, 1988

PUBLIC SERVICE ELECTRIC AND GAS COMPANY
HOPE CREEK NUCLEAR GENERATING STATION

GRAPHIC REPRESENTATION OF TYPICAL TORUS ATTACHED PIPING SYSTEM

UPDATED FSAR

Appendix 3B
FIGURE II-3

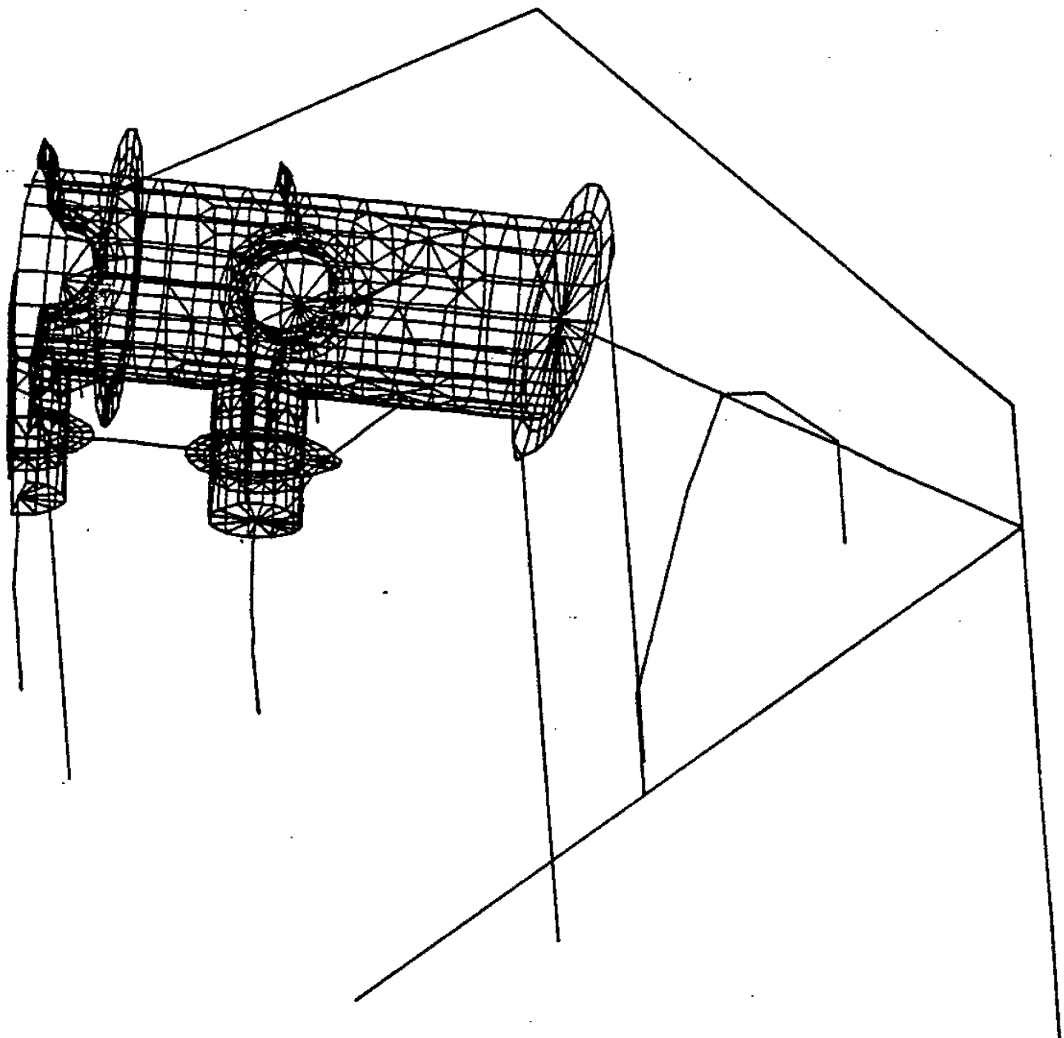

REVISION 0
APRIL 11, 1988

PUBLIC SERVICE ELECTRIC AND GAS COMPANY
HOPE CREEK NUCLEAR GENERATING STATION

VENT SYSTEM
FINITE ELEMENT MODEL
ISOMETRIC VIEW

UPDATED FSAR

Appendix 3B
FIGURE VI-1

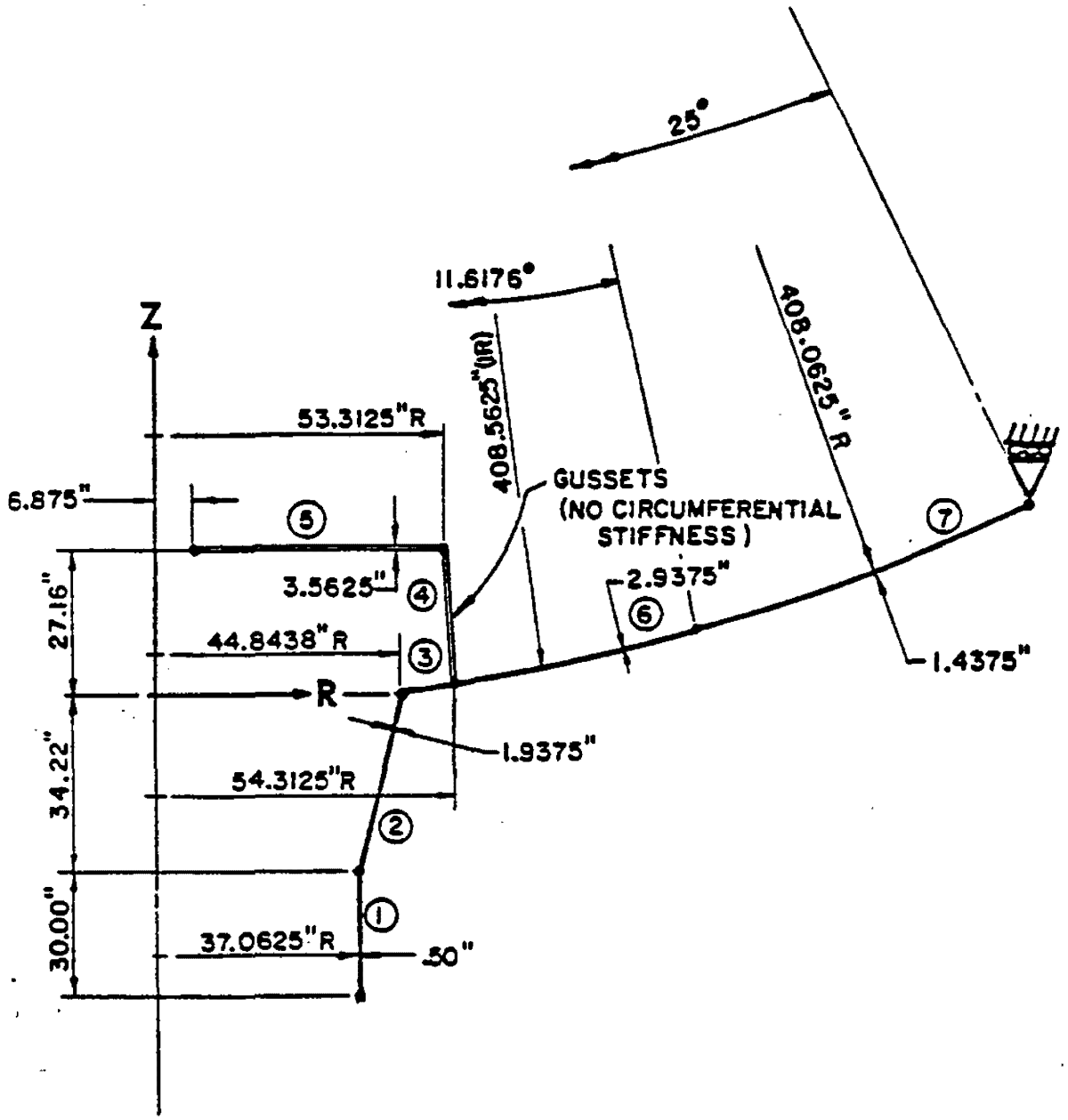

REVISION 0
APRIL 11, 1988

PUBLIC SERVICE ELECTRIC AND GAS COMPANY
HOPE CREEK NUCLEAR GENERATING STATION

FINITE DIFFERENCE MODEL
OF VENT LINE –
DRYWELL INTERSECTION

UPDATED FSAR

Appendix 3B
FIGURE VI-2

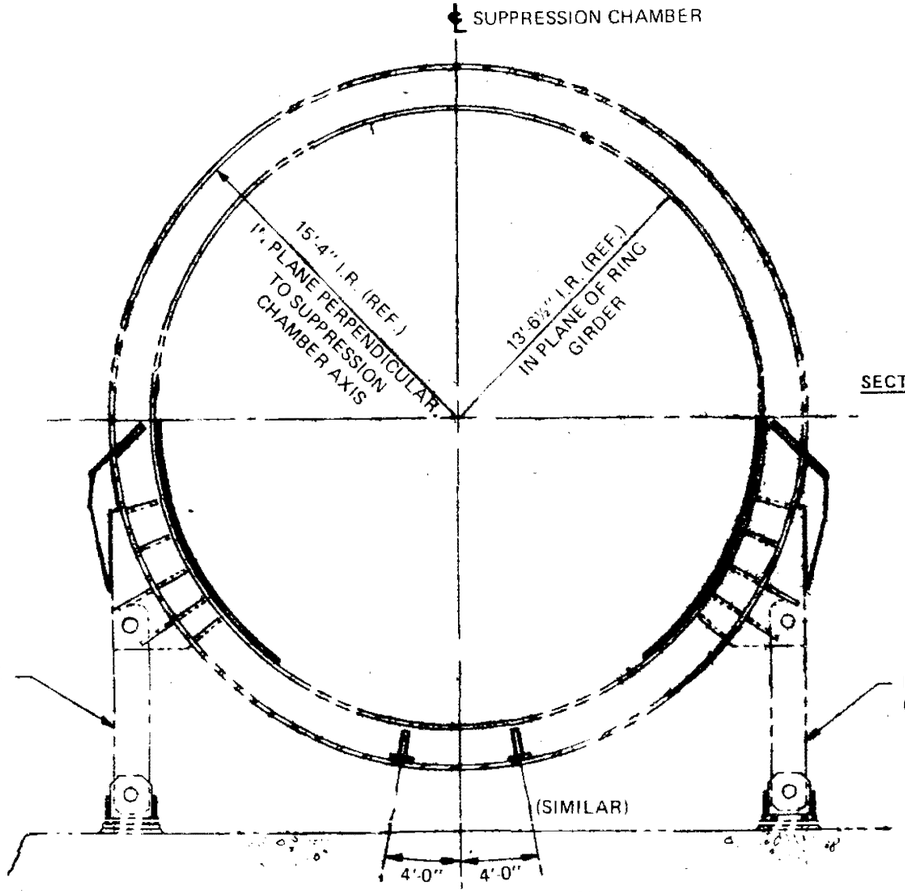

SECTION AT MITERED JOINT

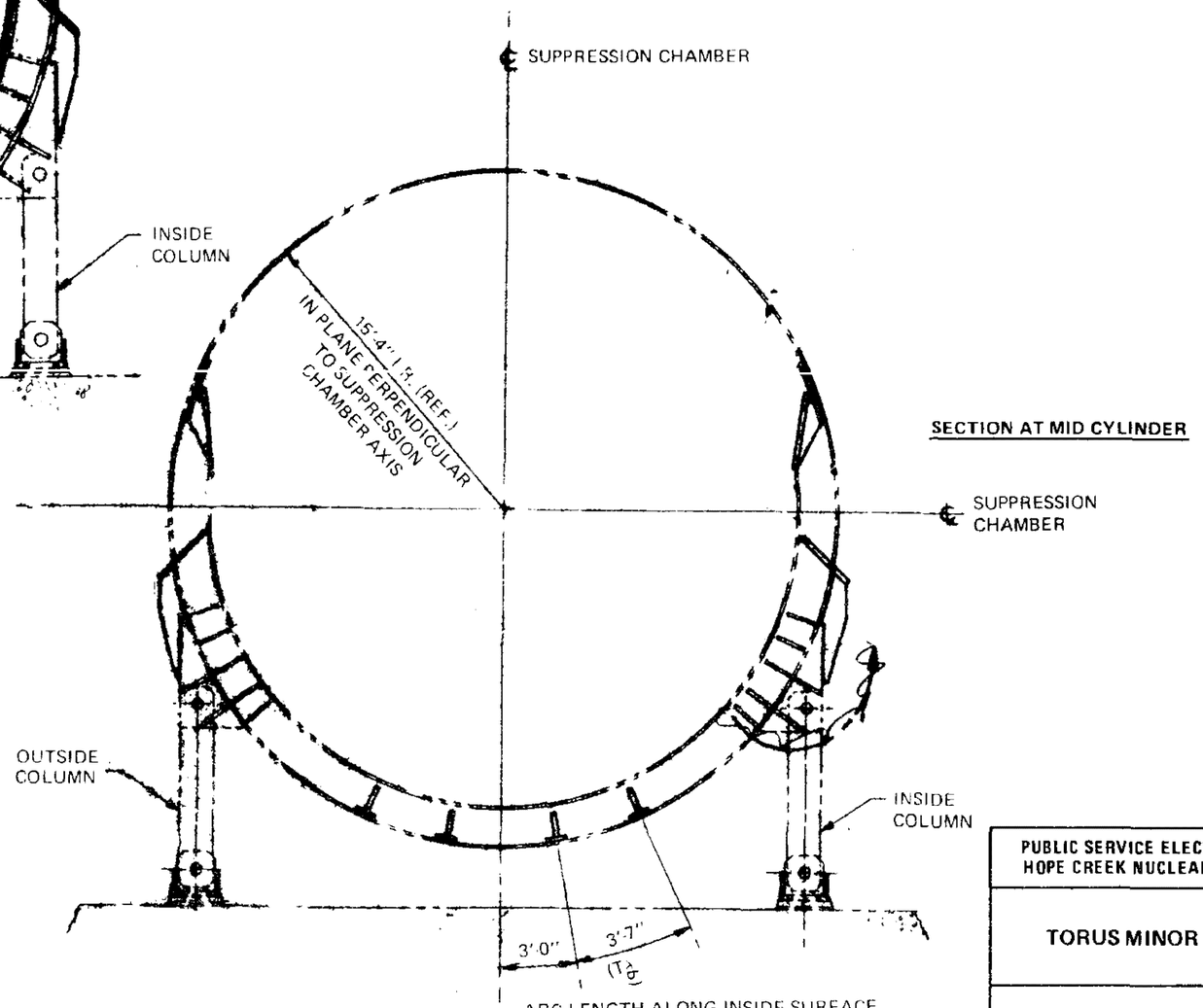

SECTION AT MID CYLINDER

REVISION 0
APRIL 11, 1988

PUBLIC SERVICE ELECTRIC AND GAS COMPANY
HOPE CREEK NUCLEAR GENERATING STATION

TORUS MINOR MODIFICATIONS

UPDATED FSAR

Appendix 3B
FIGURE VII-1

APPENDIX 3C

REACTOR ASYMMETRIC LOADS ANALYSIS *

Dynamic system analyses are performed to confirm the structural design adequacy of the reactor internals and the reactor coolant piping (unbroken loops) to withstand the dynamic loadings of the most severe loss-of-coolant accident (LOCA) and safe shutdown earthquake (SSE). The SSE analysis is described in Section 3.7. LOCA structural analysis is described in this appendix. The thermal hydraulic analysis of a LOCA is described in Section 6 and the resulting pressure differentials on core structures are discussed in Section 3.9.5.2.

Reactor asymmetric loads following a LOCA affect the structural design of the reactor internals and coolant piping. These loads result from a pipe break at the reactor nozzle safe end to pipe weld. The four components of the loads are shown on Figure 3C-1 for a postulated break; the feedwater line and recirculation line breaks have been found to be controlling.

The four components of the asymmetric loads are:

1. Asymmetric annulus pressurization loads - For each break, the pressure time histories in the annulus are calculated using the COPDA computer code. A pipe break is assumed, and the flow into the annulus is calculated. The results are pressure time histories on the biological shield and the reactor vessel. Details of the thermal hydraulic analysis are given in Section 6.

(*) As part of the MELLLA evaluation, the reactor asymmetric loads due to Feedwater Line Break (FWLB) and Recirculation Suction Line Break (RSLB) were re-evaluated. The FWLB Annulus Pressurization Load was evaluated based on the mass/energy release consistent with MELLLA and it was concluded that the original licensing basis FWLB loads bounded the MELLLA condition.

The Recirculation Suction Line Break (RSLB) Annulus Pressurization loads in the MELLLA condition, calculated based on the original methodology, were not bounded by the original design basis. Therefore, improvements to the responses using the improved methodologies were made. Based on the load responses using the improved methodologies for the MELLLA condition, it was concluded that the MELLLA condition responses were bounded by the original design basis. The description of the revised methodologies for the reactor asymmetric RSLB loads used in the MELLLA condition evaluation are presented subsequently in this Appendix 3C, under the heading "Evaluation of RSLB Reactor Asymmetric Loads in the MELLLA condition."

2. Jet reaction load on the reactor vessel - A steady state value of the jet reaction load is calculated, and it is conservatively assumed that this value is reached in 1 millisecond. This load acts at the centerline of the nozzle where the break has occurred.

3. Jet impingement loads - The full impingement force from the broken pipe flow is considered to impact against the reactor pressure vessel (RPV) and the biological shield at the elevation of the nozzle break. The geometry of the biological shield opening opposite the affected nozzle determines the proportion of jet impingement from the nozzle on the biological shield. The impingement force is derived from a pipe whip analysis of the affected pipe system and is conservatively assumed to reach full value in 1 millisecond.

4. Pipe whip restraint loads - The loads on the biological shield from the pipe whip restraints are also derived from the respective pipe whip analysis. This load is generally modeled as being zero until the pipe impacts the restraints. The load quickly rises to a peak restraint load and then drops to a steady state force. This analysis also demonstrates the ability of the pipe whip restraints to hold the broken pipe within the biological shield and annulus.

The structural dynamic analysis of the reactor asymmetric loads considers the above four loads. These are resolved to the proper nodes of the mathematical model and a time history analysis is performed. The resultant forces and moments are used to evaluate the RPV and internals. The resultant acceleration time histories are used to generate response spectra, and these are used to analyze the piping.

The theory, methods, and computer codes used for dynamic analysis of the RPV, internals, the surrounding structures, and for the attached piping are the same as those used for the seismic analyses, and are described in Sections 3.7 and 3.9.1.2. The mathematical models used for the piping analyses are the same as

those used for seismic analyses. The mathematical model used for analysis of the RPV and surrounding structures is a reduced version of the seismic model, since the reactor asymmetric loads are local loads.

The codirectional dynamic forces from the SSE and reactor asymmetric loads analyses are combined by the square root of the sum of the squares (SRSS) method. The resultant SRSS forces are combined with the quasi steady state LOCA pressure differential load and static loads on an absolute-sum basis, to determine the loads for evaluation of reactor vessel and core structures. Section 3.9.5.2 describes the hydrodynamic analysis method for determining the pressure differentials.

Evaluation of faulted conditions, for the reactor internals, including the core support structures, is described in Section 3.9.1.4 and summarized in Tables 3.9-4b and 3.9-4c. The effects of suppression chamber dynamic loads due to the LOCA are discussed in Table 3.9-4a. The effects of compressive loads due to the SSE and the compressive loads or the overturning moments and shears due to the reactor asymmetric loads are included in the evaluation.

Evaluation of RSLB Reactor Asymmetric Loads in the MELLLA condition

The reactor asymmetric loads due to RSLB were evaluated in the MELLLA conditions. The AP mass and energy release analysis was performed over the range of power/flow conditions associated with the MELLLA boundary, i.e., rated conditions at NFWT, rated conditions with FWTR, MELLLA conditions with FWTR, and MELLLA minimum pump speed with FWTR (which represents the maximum fluid subcooling).

The AP loads, the jet reaction loads/jet impingement loads, and the pipe whip loads would occur during the time periods following the double ended guillotine break of the recirculation suction line, and are combined for the evaluation of the structural integrity of the RPV, reactor internals, the biological shield wall, control rod drive (CRD) mechanisms, and the piping systems that are connected to the RPV and penetrate the biological shield wall. The results of the RSLB evaluation at the bounding condition (MELLLA minimum pump speed with FWTR) are discussed below.

1. Annulus Pressurization Load - Revised Methodology

The original methodology for calculating the mass/energy release profile for AP loads was conservative. Using this methodology, the mass and energy release profile calculated for MELLLA exceeds the HCGS design calculations. Therefore, for the MELLLA analysis, a more realistic blowdown mass and energy release profile was determined using the GE code LAMB for the RSLB AP load analysis. The LAMB [Reference 3C-1] code considers the pipe break separation time history, but ignores the fluid inertia effect, providing conservative results.

Based on the mass and energy data generated using LAMB, the AP pressure time histories on the RPV and shield wall were generated using the COMPARE code [Reference 3C-2], taking into consideration the existing 25/75 flow diverter which limits the break flow into the annulus to a nominal value of 25%.

2. Jet Reaction/Jet Impingement load - Refined Methodology

The same pipe break separation time history used for the mass and energy release calculations for the AP load above is used to calculate the jet reaction/jet impingement loads on the RPV and the biological shield wall.

The original methodology for calculating the RSLB jet reaction/jet impingement loads on the RPV and the biological shield wall is conservative. This methodology assumes a 1.0 millisecond rise time to the steady state loads. However, using this methodology causes the net effect of the AP, jet reaction, and jet impingement loads calculated for MELLLA to exceed the HCGS design calculation. Therefore, a more realistic, but still conservative refinement to the method was made to define these jet loads as a function of time. While the jet reaction/jet impingement load on the RPV has a sudden rise at the moment of the RSLB (because the RPV is the source of the high pressure fluid), the biological shield wall does not experience the jet reaction/jet impingement load until the flow diverter is pressurized by the break flow. The flow rates in the recirculation suction nozzle, in the break itself, and in the flow diverter, were calculated at the critical flow condition using the Moody Homogeneous Equilibrium Model (HEM) [Reference 3C-3]. This calculation is conservative, because it assumes that the flows in the recirculation suction nozzle, the recirculation pipe on the side of the recirculation pump, and the flow diverter are established instantaneously, i.e., reach the quasi-steady state values, for a given RSLB pipe separation at each time step as if there is no inertia in the fluid. The calculational procedure followed ANSI/ANS-58.2-

1988 (i.e., the loads were calculated at discrete times using Equation 6-2), and the guidelines provided in paragraphs (2) and (3) of Section III.2.c of Standard Review Plan (SRP) 3.6.2.

3. Pipe Whip Restraint Load

A comparison was made between the magnitude of the currently existing analysis pipe reaction load at the postulated break in the recirculation suction pipe near the RPV nozzle, and the recalculated pipe reaction load that included the effect of MELLLA and the flow diverter. It was concluded that the recalculated pipe reaction force magnitude at steady state conditions is within the acceptable range of the currently existing analysis magnitude. The existing analysis included sufficient conservatism in the piping geometry to off-set the higher force evaluated for the MELLLA condition. Therefore, thecalculated values of pipe whip restraint force and the pipe displacement profile as a function of time, developed in the currently existing analysis, remain applicable in the MELLLA condition.

Structural Response Evaluation for MELLLA

The RSLB loads based on the revised methodologies described above were applied to the combined structural model, which included the RPV, vessel internals, CRD mechanism, shield wall, and reactor building. The structural responses resulting from this load application in the MELLLA condition (forces and moments, peak accelerations, and acceleration response spectra) were compared to the original design basis. Based on this comparison, it was concluded that the MELLLA-based combined responses of the AP, jet reaction, jet impingement, and pipe whip restraint loads, which form the load input to the RPV, vessel internals, CRD mechanism, shield wall, and main steam and recirculation piping, are bounded by those of the original design basis.

References:

3C-1 NEDO-20566A, "General Electric Company Analytical Model for Loss-of-Coolant Analysis in Accordance with 10CFR50 Appendix K," September 1986.

3C-2 COMPARE-MOD 1 A "Code for Transient Analysis of Volumes with Heat Sinks, Flowing Vents and Doors" LA-7199-MS, Parsons E&C.

3C-3 Letter, D. Eisenhut (NRC) to L. J. Sobon (GE), "Review of General Electric Topical Report NEDO-21052, "Maximum Discharge Rate of Liquid-Vapor Mixtures from Vessels," MFN-004-79, December 27, 1978. [with enclosed Topical Report Evaluation - NEDO-21052].

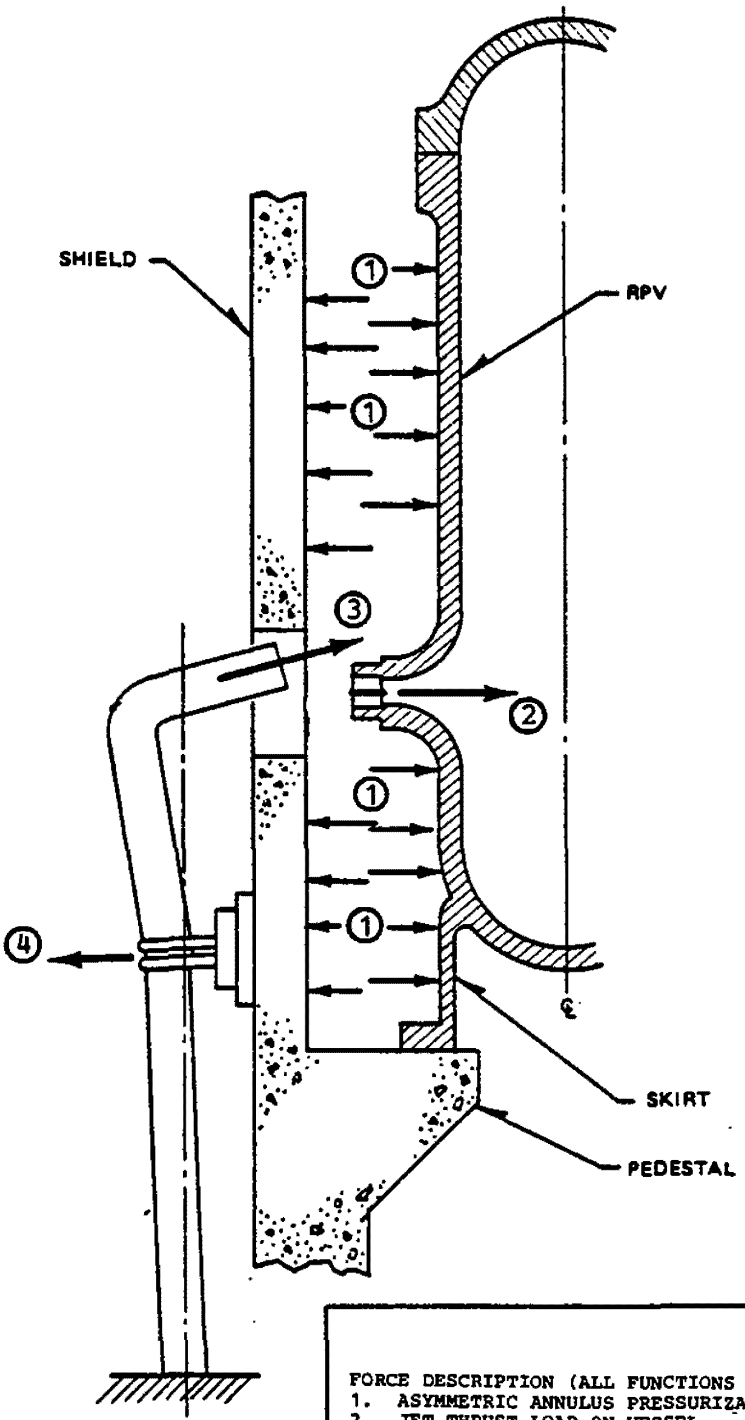

FORCE DESCRIPTION (ALL FUNCTIONS OF TIME)
1. ASYMMETRIC ANNULUS PRESSURIZATION LOAD
2. JET THRUST LOAD ON VESSEL
3. JET IMPINGEMENT LOADS
4. PIPE WHIP RESTRAINT LOAD ON SHIELD WALL

REVISION 0
APRIL 11, 1988

PUBLIC SERVICE ELECTRIC AND GAS COMPANY
HOPE CREEK NUCLEAR GENERATING STATION

LOADING DESCRIPTION

UPDATED FSAR

FIGURE 3C-1

APPENDIX 3D

FOUNDATION MAT DESIGN

3D.1 OVERVIEW

Critical sections, loads and method of accommodation of loads for the Reactor Building and southern section of the radwaste/service area (referred to herein as the Reactor Building), and Auxiliary Building control/diesel generator and central section of radwaste/service area (referred to herein as Auxiliary Building) basemat will be presented.

3D.2 REACTOR BUILDING BASEMENT - CRITICAL SECTIONS AND LOADS

A plot of the Reactor Building Basemat computer model is shown on Figure 3D-1. The critical sections for the Reactor Building basemat occur under the drywell pedestal, as represented by elements 1 through 8 on Figure 3D-1.

Load combination $1.4D + 1.7L + 1.0F_1$ (F_1 is load due to post accident containment flooding) governs the flexural reinforcing requirements for the Reactor Building basemat. Table 3D-1 lists the moments and axial forces for elements 1 through 8.

Load combination $1.4D + 1.7L_0 + 1.9E_0$ governs the shear reinforcing requirements for the reactor building basemat. Table 3D-2 lists the shears for elements 1 through 8.

3D.3 AUXILIARY BUILDING BASEMAT - CRITICAL SECTIONS AND LOADS

A plot of the Auxiliary Building basemat computer model is shown on Figure 3D-2. The critical sections for various load combinations are represented by elements 1 through 16 on Figure 3D-2.

Load combination $1.4D + 1.7L_0 + 1.9E_0$ governs the top flexural reinforcing requirements for the Auxiliary Building basemat. Table 3D-3 lists the moments and axial forces for elements 1 through 8. The forces in the y-direction control design.

Load combination 1.4D + 1.7L governs the bottom flexural reinforcing requirements for the Auxiliary Building basemat. Table 3D-4 lists the moments and axial forces for elements 9 through 16. The forces in the y-direction control design.

Load combination $1.4D + 1.7L_0 + 1.9E_0$ governs the shear reinforcing requirements for the Auxiliary Building basemat. Table 3D-5 lists the shears for elements 1 through 8.

3D.4 ACCOMMODATION OF LOADS IN BASEMAT DESIGN

As shown in Figures 3.8-40 and 3.8-42, the Reactor Building and Auxiliary Building basemats have been provided with flexural and shear reinforcing to accommodate design loads as required by the strength method of the ACI-318 code.

For each load case considered in the design of the basemats, required flexural and shear reinforcing was determined for each element in the applicable basemat model corresponding to the loads acting on that element and mapped on the basemat models. A composite map for each basemat was generated, indicating the controlling reinforcing required for each element of the basemat model. From these composite maps, the flexural and shear reinforcing layouts were made.

Since the basemats were constructed in two seven foot lifts, horizontal shear at the mid-depth of the basemats was checked in accordance with Section 17.5 of the ACI-318 code. The pits and sumps in the basemats were designed in accordance with Section 13.6 of the ACI-318 code. The reinforcing steel interrupted by an opening for a pit or sump is replaced on the sides of the opening.

TABLE 3D-1

AXIAL FORCES AND MOMENTS FOR REACTOR BUILDING BASEMAT ELEMENTS UNDER DRYWELL PEDESTAL FOR LOAD COMBINATION $1.4D + 1.7L + 1.0F_1$

	X-Direction		Y-Direction	
Element No.*	Axial Force (Kips)	Moment (K-ft)	Axial Force (Kips)	Moment (K-ft)
1	377.9	2,043.1	473.4	1,953.9
2	448.4	1,327.9	487.6	1,487.7
3	464.8	1,415.1	494.2	1,550.7
4	428.9	2,359.1	488.6	2,154.9
5	389.0	2,207.3	498.9	2,273.2
6	473.3	1,503.6	524.4	1,781.2
7	483.8	1,538.8	524.7	1,759.2
8	440.6	2,460.2	511.8	2,327.8

* See Figure 3D-1 for location of elements.

TABLE 3D-2

SHEARS FOR REACTOR BUILDING BASEMAT ELEMENTS UNDER DRYWELL PEDESTAL FOR LOAD COMBINATION $1.4D + 1.7L_0 + 1.9E_0$

Element No.*	Shear YZ-Direction (Kips)	Shear XZ-Direction (Kips)
1	88.1	-177.7
2	109.8	- 84.8
3	115.1	107.1
4	109.1	225.8
5	-147.7	-225.1
6	-157.5	-111.9
7	-155.4	121.1
8	-152.5	256.2

* See Figure 3D-1 for location of elements.

TABLE 3D-3

AXIAL FORCES AND MOMENTS IN Y-DIRECTION FOR ELEMENTS 1 THROUGH 8 OF THE AUXILIARY BUILDING BASEMAT FOR LOAD COMBINATION $1.4D + 1.7L_0 + 1.9E_0$

	Y-Direction	
Element No.*	Axial Force (Kips)	Moment (K-ft)
1	19.3	1,545.7
2	21.4	1,553.4
3	20.9	1,549.7
4	13.9	1,394.8
5	52.8	1,265.2
6	15.2	1,044.6
7	44.6	1,353.3
8	39.2	1,570.9

* See Figure 3D-2 for location of elements.

TABLE 3D-4

AXIAL FORCES AND MOMENTS IN Y-DIRECTION FOR ELEMENTS 9 THROUGH 16 OF THE AUXILIARY BUILDING BASEMAT FOR LOAD COMBINATION 1.4D + 1.7L

	Y-Direction	
Element No.*	Axial Force (Kips)	Moment (K-ft)
9	157.6	388.2
10	146.2	354.1
11	147.4	232.5
12	156.9	125.6
13	182.0	179.9
14	141.1	293.3
15	107.9	369.2
16	195.6	450.3

* See Figure 3D-2 for location of elements.

TABLE 3D-5

SHEAR FORCES FOR ELEMENTS 1 THROUGH 8 OF THE AUXILIARY BUILDING BASEMAT FOR LOAD COMBINATION $1.4D + 1.7L_0 + 1.9E_0$

Element No.*	Shear XZ-Direction (Kips)	Shear YZ-Direction (Kips)
1	5.9	13.4
2	9.4	14.6
3	33.5	14.4
4	64.8	21.6
5	19.0	49.7
6	9.2	56.3
7	35.1	60.8
8	51.1	113.5

* See Figure 3D-2 for location of elements.

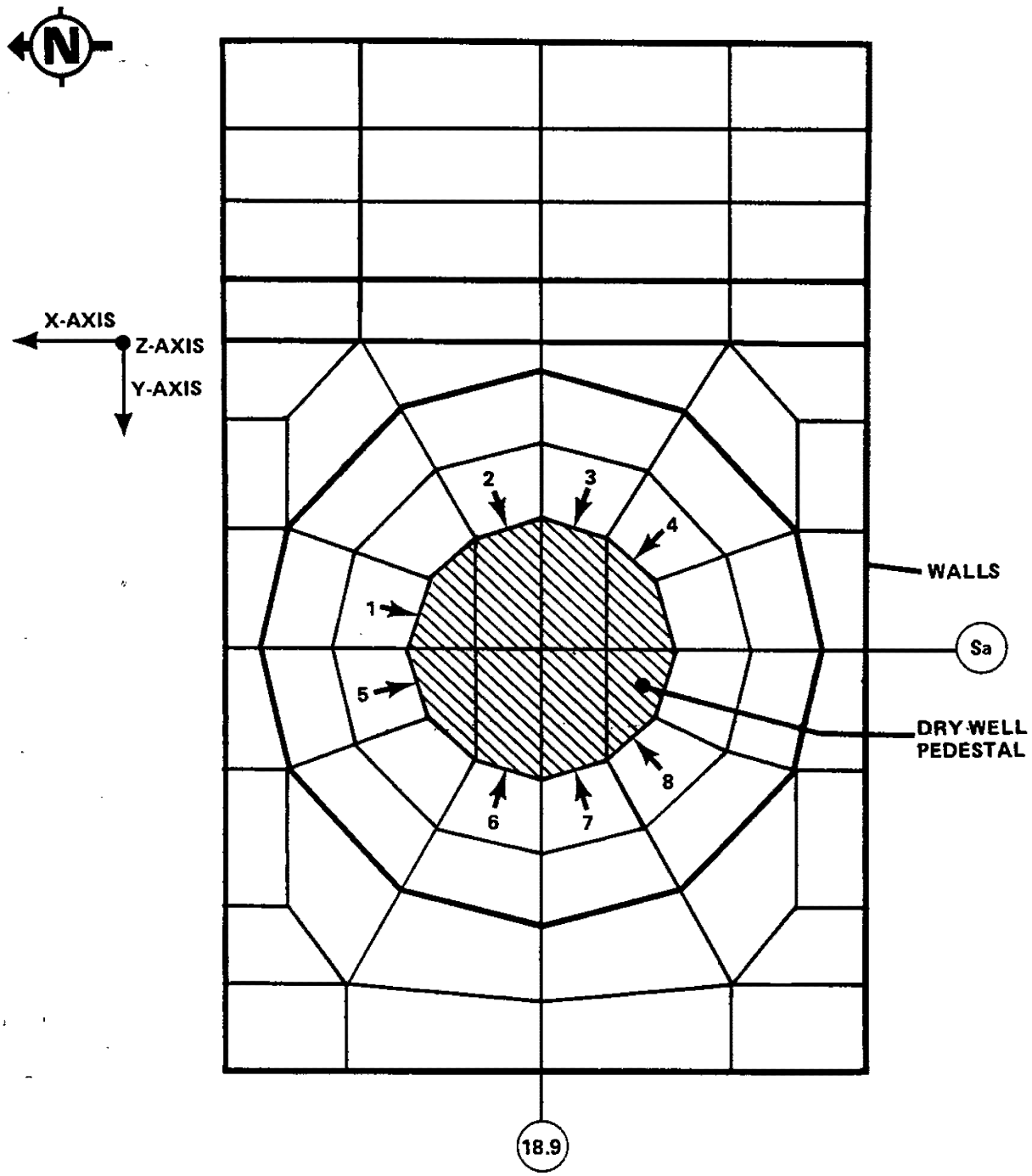

PLAN- REACTOR BUILDING ONLY

REVISION 0
APRIL 11, 1988

PUBLIC SERVICE ELECTRIC AND GAS COMPANY
HOPE CREEK NUCLEAR GENERATING STATION

PLOT OF REACTOR BUILDING
BASEMAT COMPUTER MODEL

UPDATED FSAR

FIGURE 3D-1

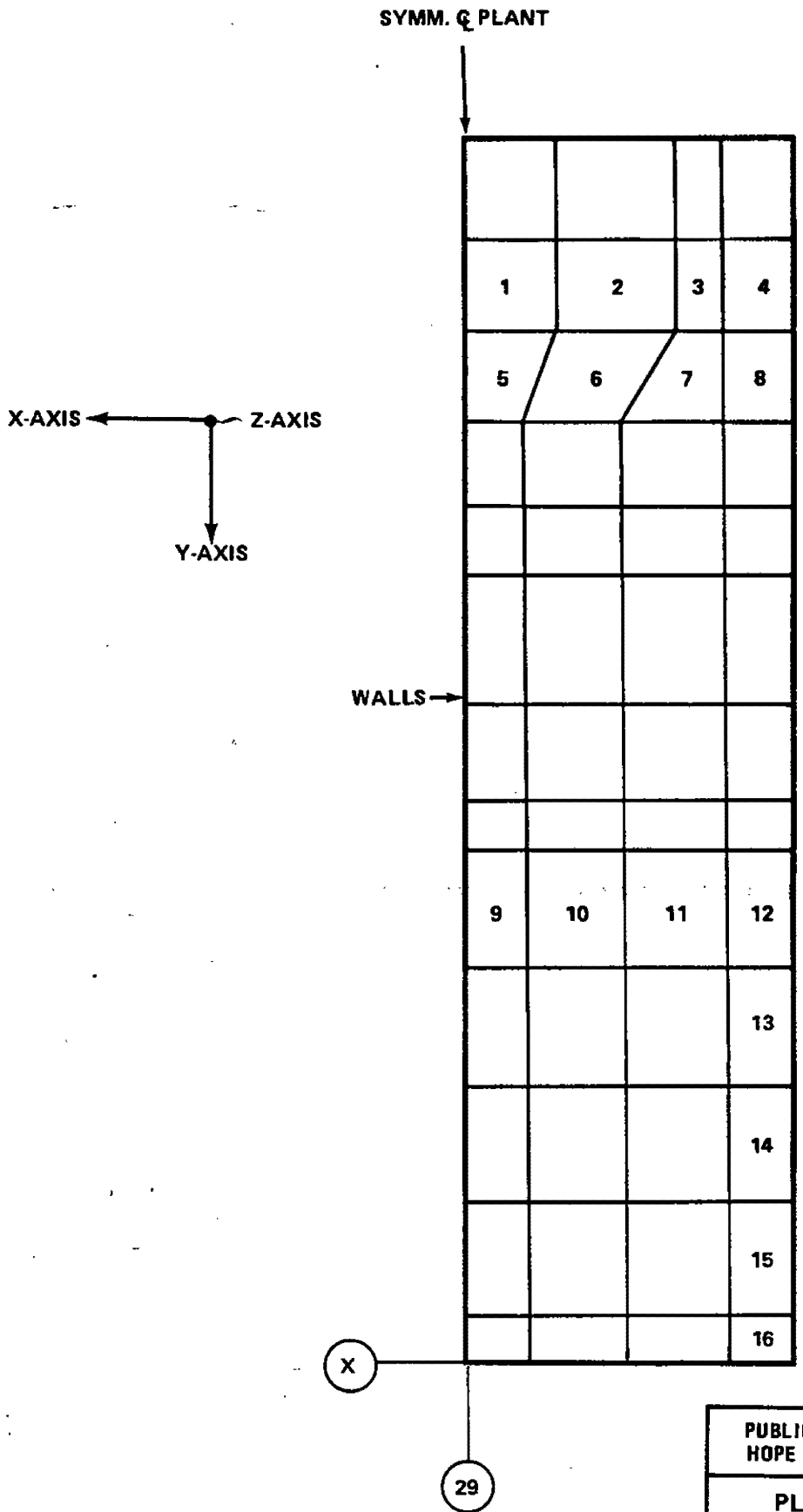

REVISION 0
APRIL 11, 1988

PUBLIC SERVICE ELECTRIC AND GAS COMPANY
HOPE CREEK NUCLEAR GENERATING STATION

PLOT OF AUXILIARY BUILDING CONTROL/DIESEL GENERATOR BASEMAT COMPUTER MODEL

UPDATED FSAR

FIGURE 3D-2

APPENDIX 3E

BUCKLING ANALYSIS OF THE DRYWELL VESSEL

3E.1 EVALUATION

The analytical model shown on Figure 3.8-18 is used to perform the buckling analysis of the drywell shell for all enveloping load combinations.

As discussed in Section 3.8.2.4.1, the drywell is analyzed as an axisymmetric shell model subjected to loads which account for both axisymmetric or non axisymmetric loads. The shell is embedded in concrete below elevation 1041.9 inches and is therefore assumed to be fixed at this point. Above this elevation, it is separated from the drywell concrete shield wall by a 2-inch air gap and therefore is considered free standing.

The loading combinations considered in the design of the drywell shell are listed in Table 3.8-2.

An examination of the load combinations reveals that it is not necessary to evaluate compressive stresses for all load combinations, since some are enveloped by others. For example, loading combinations containing internal pressure will reduce compressive stresses and are therefore of less concern for buckling. The enveloping load combinations for buckling analysis are listed in Table 3E-1.

The critical compressive stresses at buckling for the drywell sphere are determined by performing a linear bifurcation buckling analysis using the BOSOR4 computer program. The buckling analyses are performed to determine the lowest eigenvalue for the compressive loads specified for each enveloping load combination.

The buckled mode shape is evaluated to determine the location at which buckling of the drywell shell occurs. The compressive stresses at this location are divided by a factor of safety which is equal to the ratio of the theoretical buckling pressure for a perfect sphere to the ASME Code allowable external pressure. See note 3 of Table 3E-1.

The compressive stresses calculated by applying the actual design loads for each enveloping load combination are compared with the corresponding allowable compressive stresses to determine adequacy.

Based on the results of these analyses it was found that the critical stresses in spherical part, Segment 9, (Figure 3.8-18) occur at meshpoints 19 (elevation 1157.4) and 66 (elevation 1543.2). The stress levels from these meshpoints for enveloping load combinations along with corresponding factor of safety are listed in Table 3E-1.

To demonstrate the adequacy of the cylindrical portion of the drywell for compressive loadings, the rules of NE-3133 are used. Accordingly, the allowable external pressure for the 7/8 inch thick cylinder is 7.91 psi. Since the maximum external pressure specified for any loading combination is 3.0 psi (see Section 3.8.2.3.7), the cylindrical portion of the drywell is adequate for external pressure.

The maximum allowable compressive stress in a cylindrical shell due to axial compression loads is specified in Subparagraph NE-3133.6. For the 7/8 inch thick cylindrical shell, the allowable axial compressive stress is computed to be 6400 psi. The maximum compressive stress in the cylindrical portion of the drywell shell is calculated to be 2420 psi. Therefore, the cylindrical portion of the drywell is also adequate for axial compression.

Based on the results of BOSOR4 analysis for the remainder of the drywell shell, the compressive stresses were found to be low and therefore did not control the design.

From the preceding results it is shown that, with respect to drywell shell buckling, adequate safety margin exists.

3E.2 ADDITIONAL EVALUATION

As a follow up to NRC's comments (see Question 220.11), an additional buckling evaluation is performed for the drywell vessel.

3E.3 CRITERIA

ASME Code Case N-284 is used for this evaluation with the following exceptions:

1. Level A and B service limits FS = 3

2. Level C service limit FS = 2.5

3. Level D service limit FS = 2

4. 25 percent reduction in the allowable critical stress level at locations where large openings exist.

The above exceptions, though more stringent than the ASME Code Case N-284 requirements, meet the NRC's guidelines for buckling evaluation.

3E.4 LOAD COMBINATIONS

The governing load combinations are as follows;

1. $D + L + T_e + R_e + P_e + E$ level B service limit

2. $D + L + T_e + R_e + P_e + E'$ level C service limit

3E.5 SUMMARY OF RESULTS

The summary of results are listed in Tables 3E-2 and 3E-3.

3E.6 CONCLUSIONS

The containment vessel meets the intent of the Code Case N-284 as modified by the NRC.

TABLE 3E-1

BUCKLING ANALYSIS RESULTS FOR SPHERICAL
PORTION OF THE DRYWELL SHELL

LOADING COMBINATIONS (1) / BUCKLING PARAMETERS	$D+L+T_0+R_0+P_0+E$		$D+L+T_e+R_e+P_e+E$		$D+L+T_e+R_e+P_e+E'$		$D+L+F_1+T_0+R_0+E$	
Buckled Mesh Point	19	66	19	66	19	66	19	66
Calculated Stress: σa	-2510.0	-807.3	-2623.0	-1157.0	-3312.0	-1378.0	-1523.0	+1641.0
Critical Buckling Stress: σcr (2)	-78429.0	-29698.0	-78339.0	-30390.0	-78082.0	-26274.0	-78296.0	-17842.0
Required Factor of Safety: (3)	18.72	18.72	18.72	18.72	18.72	18.72	18.72	18.72
Actual Factor of Safety: $\sigma cr/\sigma a$	31.25	36.78	29.87	26.26	23.58	19.06	51.4	-----

Notes:

(1) See Table 3.8-2 for load definitions.

(2) Based on the lowest eigenvalue obtained from BOSOR4 analysis.

(3) Required factor of safety (FS) = $\frac{P_{cr\ (theoretical)}}{P_{crF\ (ASME)}}$ where:

$$P_{cr}(\text{theoretical}) = \frac{2Et^2}{r^2\sqrt{3(1-\nu^2)}} = \frac{2 \times 27.7 \times 10^6 \times (1.4373)^2}{(408.7813)^2\sqrt{3(1-0.3^2)}} = 414.63 \text{ psi}$$

$$P_{cr}(\text{ASME}) = \frac{B}{R/t} \qquad B = 6300 \text{ psi from Sec. NE-3133.4}$$

$$= \frac{6300}{408.7813/1.4373} = 22.15 \text{ psi}$$

$$\text{Required FS} = 414.63/22.15 = 18.72$$

TABLE 3E-2

RESULTS OF ADDITIONAL EVALUATION

Location	Load Comb.	$D + L_S + T_e + R_e + P_{eS} + E$		$D + L_S + T_e + R_e + P_{eS} + E'$		
Spherical Shell El. 88 feet-4 inch	Calculated Stress (psi)	53,749	35,119	61,183	45,635	See Note 1 and Note 3
	Allowable Stress (psi)	68,300	59,145	68,300	59,145	
Hatch Area El. 107 feet-0 inch	Calculated Stress (psi)	17,696	15,290	15,701	12,605	See Note 2
	Allowable Stress (psi)	44,358	44,358	44,358	44,358	
Cylindrical Shell El. 144 feet-4 inch	Calculated Stress (psi)	7,358	3,126	7,083	2,656	
	Allowable Stress (psi)	60,438	4,895	60,438	4,895	

Notes:

1) The calculated stresses include the stress magnification factors as specified in Code Case N-284 and safety factors (FS) as required by NRC. (FS = 3 for level B service limit and FS = 2.5 for level C service limit) and are based on stress levels obtained from BOSOR4 output.

2) The allowable stresses include 25 percent reduction as required by NRC.

3) S_S = stresses in the meriditional direction.
   S_S = stresses in the circumferential direction.

TABLE 3E-3

RESULTS OF ADDITIONAL EVALUATION

Location	Minimum Calculated Factors of Safety: Level B Service Limits	Level C Service Limits
Spherical Shell	3.8	2.8
Hatch Area	7.5	7.0
Cylindrical Shell	4.7	4.6

Note:

The above values are based on results given in Table 3E-2 and exceed the following allowable factors of safety:

- Level B Service Limits, FS = 3
- Level C Service Limits, FS = 2.5

APPENDIX F

ANALYSIS AND DESIGN OF FUEL POOL LINER AND SLAB

3F.1 SCOPE

This appendix covers loads, load combinations, analysis procedures, and acceptance criteria used for the design of the fuel pool liner and slab.

3F.2 LOADS AND LOAD COMBINATIONS

The purpose of the fuel pool liner is to provide "water tightness" to the fuel pool. Conservatively, the increased structural strength of the composite concrete slab due to the anchored liner is not considered in the design of the fuel pool slab. However, the liner is designed to withstand all loads due to construction activities, such as handling and liquid head of concrete In addition, liner plate strains and liner anchor displacements are evaluated for normal and abnormal thermal conditions.

The load combinations used in the design of the fuel pool slab are provided in Section 3.8.4.3 In addition, effects of the construction loads due to the staged construction of the side walls are considered.

The controlling load combination for the fuel pool slab is $1.4D + 1.7L_0 + 1.9E_0$ with definitions as follows:

D = Slab dead load and weight of fuel pool water

L_0 = Effective weight of fuel (fuel weight less buoyancy)

E_0 = Seismic OBE including sloshing effect of water.

A heavy load drop accident over the fuel pool slab has been precluded by provisions in Section 9.1.5 However, the potential drop of a fuel bundle during handling operations has been evaluated.

3F.3 ANALYSIS PROCEDURE

The fuel pool liner has been designed as a stiffened plate with stiffeners in both horizontal and vertical directions. Where attachment loads are considered, specially designed inserts with shear bars and tension lugs are provided. Before concrete placement the inserts are seal welded to the liner to provide water tightness. For normal and abnormal thermal conditions, liner plate strains are calculated considering the difference in coefficient of thermal expansion between the concrete and the steel liner plate. Liner anchor displacements resulting from liner plate thermal strains are calculated using the methodology given in Reference 3.8-7.

The main features of the fuel pool slab design are as follows:

1. The slab is designed for two way action with the edges supported by the side walls.

2. Additionally, the side walls of the fuel pool are designed as deep girders transferring the loads to the cylinder and the drywell shield walls, as shown in Plant Drawing P-0046-1. The bending effects of these walls on the effective width of the slab are also considered.

3. Consideration is given to the reduced shear capacity of the slab at the slab/wall interface due to existence of the tensile stress.

4. Thermal effects (axial and bending) are considered for the condition where pool water boils.

3F.4 ACCEPTANCE CRITERIA

The liner is designed for construction loads in accordance with the acceptance criteria given in Section 3.8.4.5.2 In order to minimize the potential for leakage, no increase in the allowables is permitted. In addition, for normal and abnormal thermal conditions liner plate strains and liner anchor displacements are not to exceed the allowables of ASME, B&PV Code, Section III, Division 2.

The acceptance criteria for the fuel pool slab is provided in Section 3.8.4.5.1.

3F.5 SUMMARY OF RESULTS

Table 3F-1 contains a comparison between calculated and allowable values of liner plate strains and liner anchor displacements for normal and abnormal thermal conditions.

TABLE 3F-1

LINER PLATE STRAINS AND LINER ANCHOR DISPLACEMENTS
FOR NORMAL AND ABNORMAL THERMAL CONDITIONS

1. Liner plate strains

Condition	Liner Plate Strain (in./in.) Calculated	Allowable[1]
Normal	0.000248	0.002
Abnormal	0.001013	0.005

2. Wall liner anchor displacements[4]

Condition	Liner Anchor Displacements (in.) Calculated	Allowable[2]
Normal	0.0057	0.25 σu[3] = 0.031
Abnormal	0.0206	0.50 σu[3] = 0.062

(1) From ASME B&PV Code, Section III, Div. 2, 1983 edition, Table CC-3720-1.

(2) From ASME B&PV Code, Section III, Div. 2, 1983 edition, Table CC-3730-1.

(3) $(\sigma u)_{min.}$ = 0.125 in. from test results given in Appendix B of Reference 3.8-7.

(4) Floor liner anchors have no displacement due to hydrostatic pressure.

APPENDIX 3G

INTAKE STRUCTURE STABILITY ANALYSES

I. Overview

Load combinations, key assumptions, and summary of safety factors for the intake structure stability analyses will be presented. Figure 3G-1 shows the intake structure and surrounding area.

II. Load Combinations

The load combinations listed in Section 3.8.5.3, which are consistent with SRP Section 3.8.5-II of NUREG-0800, were considered for the stability analyses of the intake structure.

The design basis flood combination, D + F, controls the factor of safety calculation for floatation.

The load combination D + H + E controls the factor of safety calculations for sliding and overturning.

III. Key Assumptions

The key assumption for the floatation check during the design basis flood is that the buoyancy force is based on the maximum still water level of Elevation 113.8 feet, as shown in Table 2.4-10. This assumption is consistent with the requirements of SRP Section 3.4.2 of NUREG-0800.

Key assumptions for the sliding and overturning check during an SSE event are as follows:

1. Soil layers and properties are based on information discussed in Section 2.5.

2. As indicated in Section 2.5.4.8.3 concerning liquefaction potential, the only soils which could liquefy during an SSE event are the sandy portion of the hydraulic fill, which occur generally in the upper 30 feet at the site. However, for conservatism, it is assumed that the entire hydraulic fill layer where it exists on the landward side of the intake structure will liquefy during an SSE event.

3. In evaluating side wall friction (x), the resistance due to hydraulic fill is neglected.

4. Conservatively, the ground water table is located at the final grade level of elevation 100 feet.

5. To obtain a conservative value of unbalanced lateral loading on the intake structure, the water in the river is assumed to be at the mean low tide level of elevation 86.4 feet.

6. Since passive earth pressure is considered in the calculations, the service water piping joints have been designed with adequate flexibility to accommodate the structural movement of the intake structure.

IV. Summary of Safety Factors for Stability Checks

The factors of safety against sliding, overturning and floatation are shown on Figure 3G-2. The factor of safety against overturning given in Figure 3G-2 is calculated based on the energy method approach described in Reference 3.7-1. The factor of safety against overturning using conventional methods is 1.12. All calculated safety factors for the stability checks exceed the minimum safety factors specified by Section 3.8.5.5, which is consistent with SRP Section 3.8.5-II of NUREG-0800.

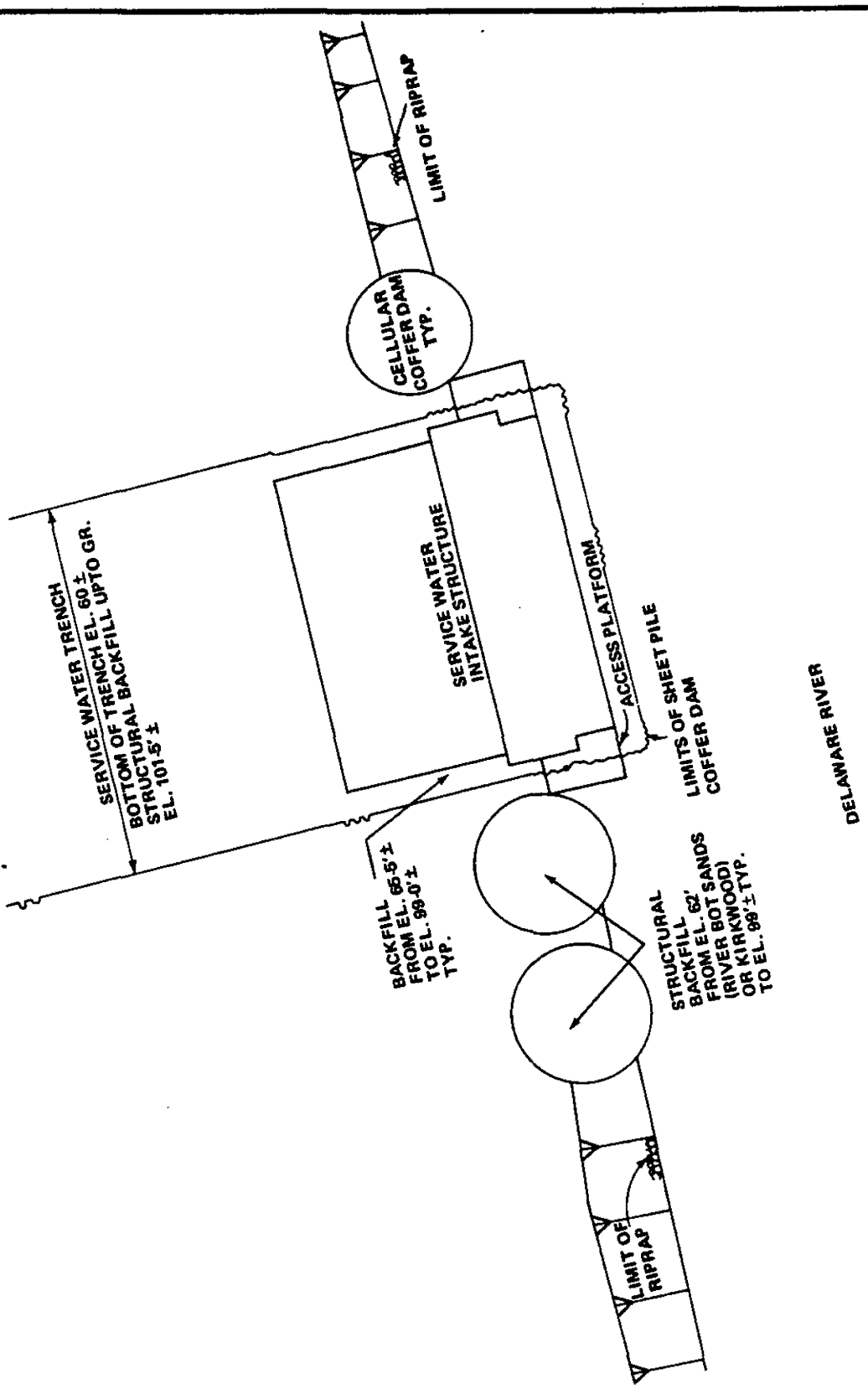

REVISION 0
APRIL 11, 1988

PUBLIC SERVICE ELECTRIC AND GAS COMPANY
HOPE CREEK NUCLEAR GENERATING STATION

INTAKE STRUCTURE
STABILITY FEATURES

UPDATED FSAR

FIGURE 3G-1

LOAD COMBINATION			
		$D + H + E_s$	$D + F$
		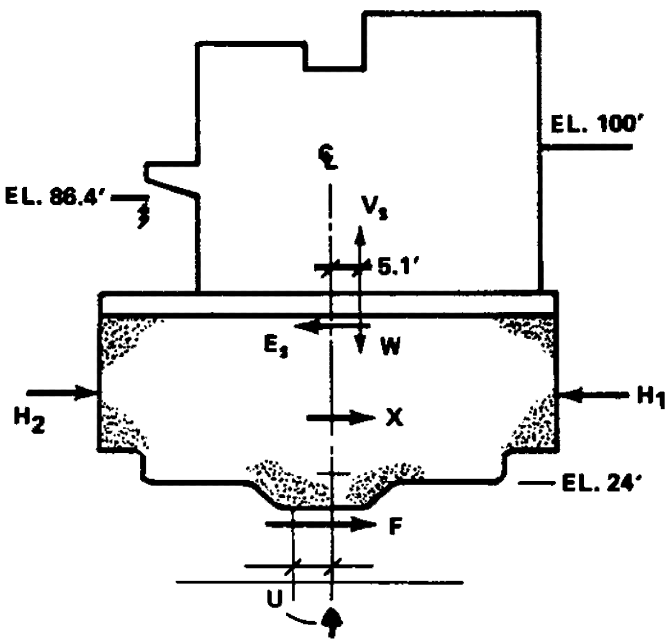	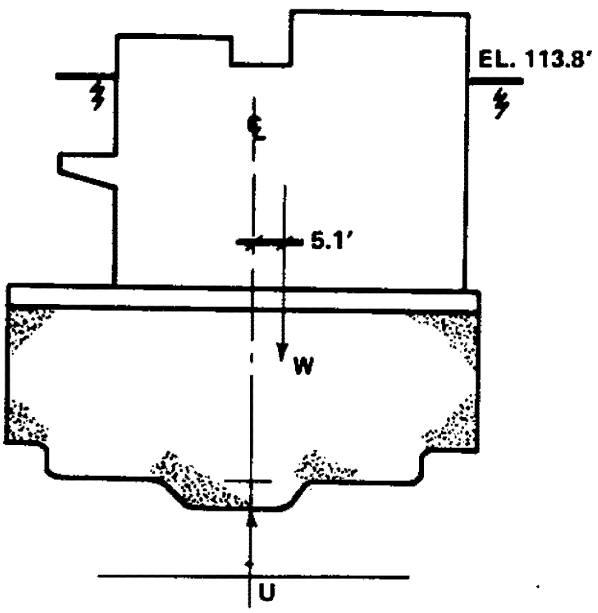
FORCES	W	106,000K	106,000K
	H_1	29,000	–
	H_2	22,760	–
	F	14,920	–
	U	75,570	69,300
	E_s	21,210	–
	V_s	8,480	–
	X	15,860	–
F.S.		OVERTURNING 710>1.1 MINIMUM F.S. SLIDING 1.12 > 1.1 MINIMUM F.S. –	– – FLOTATION 1.64 > 1.1 MINIMUM

E_s SAFE SHUTDOWN EARTHQUAKE LATERAL FORCE
F SUBGRADE FRICTION RESISTANCE
H_1 DRIVING EARTH PRESSURE
H_2 RESISTING EARTH PRESSURE
U UPLIFT DUE TO GROUNDWATER AND EXCESS PORE PRESSURE DURING SEISMIC EVENT, OR DESIGN BASIS FLOOD
V_s SAFE SHUTDOWN EARTHQUAKE VERTICAL FORCE
X TOTAL SIDE FRICTION
W DEAD LOADS

REVISION 0
APRIL 11, 1988

PUBLIC SERVICE ELECTRIC AND GAS COMPANY
HOPE CREEK NUCLEAR GENERATING STATION

SAFETY FACTORS
FOR INTAKE
STRUCTURE STABILITY CHECKS

UPDATED FSAR

FIGURE 3G-2

APPENDIX 3H

POWER BLOCK STABILITY ANALYSIS

I. OVERVIEW

Load combinations, key assumptions and summary of safety factors for the powerblock analyses are presented in this appendix. Figure 3H-1 shows the layout of the power block area.

II. LOAD COMBINATIONS

The load combinations listed in Section 3.8.5.3, which are consistent with SRP Section 3.8.5-II of NUREG-0800, are considered for the stability analyses of the structures.

The design basis flood combination, D + F, controls the factor of safety calculation for floatation.

The load combination D + H + E controls the factor of safety calculations for sliding and overturning.

III. KEY ASSUMPTIONS

The key assumption for the floatation check during the design basis flood is that the buoyancy force is based on the maximum still water level of Elevation 113.8 feet, as shown in Table 2.4-10. This assumption is consistent with the requirements of SRP Section 3.4.2 of NUREG-0800.

The key assumptions for the sliding and overturning check during an SSE event are as follows:

1. Soil layers and properties are based on information discussed in Section 2.5 and Volume 2 of FSAR Reference 2.5-79.

2. The driving force of the structure was computed from the soil structure interaction analysis described in Section 3.7.2. This, in general, represents inertia force due to peak acceleration at various levels in the structure. This is conservative, as the peak accelerations at various levels do not necessarily occur at the same time and in the same direction.

3. As indicated in Section 2.5.4.8.3, the only soils which could liquefy during an SSE event are the sandy portion of the hydraulic fill.

   The subsurface data based on the borings in this area shows the following:

   a. Eighty five percent of the hydraulic fill materials are primarily cohesive and will not be susceptible to liquefaction

   b. Zones of liquefiable sandy materials generally occur in thin lenses or discontinuous layers.

   Based on evaluation of the above data, it is estimated that the hydraulic fill surrounding the power block structures will not experience gross liquefaction that could cause mass instability of the entire hydraulic fill. Even if these localized sandy zones liquefy, they will be contained within the non-liquefiable cohesive materials.

   In addition, as shown in Figure 3.8-44, the power block is surrounded by non-liquefiable, engineered backfill. Consequently gross liquefaction of the surrounding soil is not considered in the analysis (see Section V for additional information).

4. The vertical component of the SSE is assumed to be 40 percent of the peak acceleration in the upward direction at the time of horizontal peak acceleration.

5. In estimating passive resistance 33-1/3 percent of the passive earth pressure coefficient (Kp) is used.

6. The Seismic Category I piping (such as service water piping) penetrating the exterior walls have been designed with adequate flexibility to accommodate structural movement. It is estimated that the structural movement would be less than 0.5 inch.

7. Effect of earthquake induced excess pore pressure is considered underneath the basemat.

8. The factor of safety against overturning is calculated using the energy balance method as described in Reference 3.7-1.

IV. SUMMARY OF RESULTS

The factors of safety against sliding, overturning and floatation are shown on Table 3H-1. The factor of safety against overturning given in Table 3H-1 is calculated based on the energy method approach described in Reference 3.7-1. The factor of safety against overturning using conventional methods is 1.61. The corresponding factor of safety against soil toe contact pressure failure is 3.60. These values represent the lowest of all values calculated for different buildings. All calculated safety factors exceed the minimum safety factors specified by Section 3.8.5.5 which is consistent with SRP Section 3.8.5-II of NUREG-0800.

V. ADDITIONAL EVALUATION

In response to NRC Question 241.23 the effects of liquefied upper soils is evaluated. This evaluation is based on the following assumptions:

1. The seismic stability calculations are provided for the cancelled area (Unit 2) only; the stability conditions are better for all other power block structures.

2. The driving and resisting forces on the sides of the structures are assumed to balance each other.

3. The driving force (inertia) of the structure was computed by taking the absolute sum of the products of mass and peak acceleration (computed from the SSI analyses) at various levels in the structure. In reality, the peak accelerations at various levels do not necessarily occur at the same time and in the same direction. The effective peak acceleration for no slippage case is estimated by dividing this inertia force by the weight of the structure.

4. The vertical component of the SSE is assumed to be 40 percent of the peak acceleration in the upward direction at the time of the horizontal peak acceleration.

5. The portion of the SSE loading prior to the peak horizontal acceleration is estimated to be one equivalent uniform cycle with an amplitude equal to 0.65 times the peak value for stability calculations. The static contact pressure between the base mat and the foundation soils was reduced by the dynamic pore pressure buildup estimated at the end of this one equivalent cycle.

6. The laboratory data on cyclic strength of the foundation soils was correlated to that under field conditions of

multidirectional shaking with the factor $C\gamma$ = 0.65 corresponding to normally consolidated conditions. The construction of the power block, however, involved long term dewatering and overconsolidation of the foundation soils under the total weight (without buoyancy) of the structure.

7. The period of the peak horizontal acceleration cycle is assumed to be 0.5 seconds.

8. The energy loss in damping is ignored for the calculation of relative movement (slippage) between the structure and the foundation soils.

The stability calculations were performed based on the above assumptions. The result indicate that the slippage may occur between the basemats and the foundation soils. The relative movement is expected to be less than 1/2 inch for the SSE conditions. This movement is consistent with the movement as discussed in Section III.

TABLE 3H-1

LOAD COMBINATION

		$D + H + E_s$	$D + F$
Forces	W	1.13×10^6 K	3.20×10^5 K (cancelled area)
	H_1	6.33×10^4 K	-
	H_2	2.47×10^5 K	-
	F_s	9.95×10^4 K	-
	U	9.55×10^5 K	2.76×10^5 K
	E_s	2.26×10^5 K	-
	V	9.04×10^4 K	-
	X	1.98×10^4 K	-
Factor of Safety	Overturning	2800 >1.1	
	Sliding	1.27 >1.1	Floatation 1.19 >1.1

E_s - Safe shutdown earthquake lateral force

F_s - Subgrade friction resistance

H_1 - Driving earth pressure

H_2 - Resisting earth pressure

U - Uplift due to groundwater and excess pore pressure during seismic event, or design basis flood

V - Safe shutdown earthquake vertical force

X - Total side friction

W - Dead loads

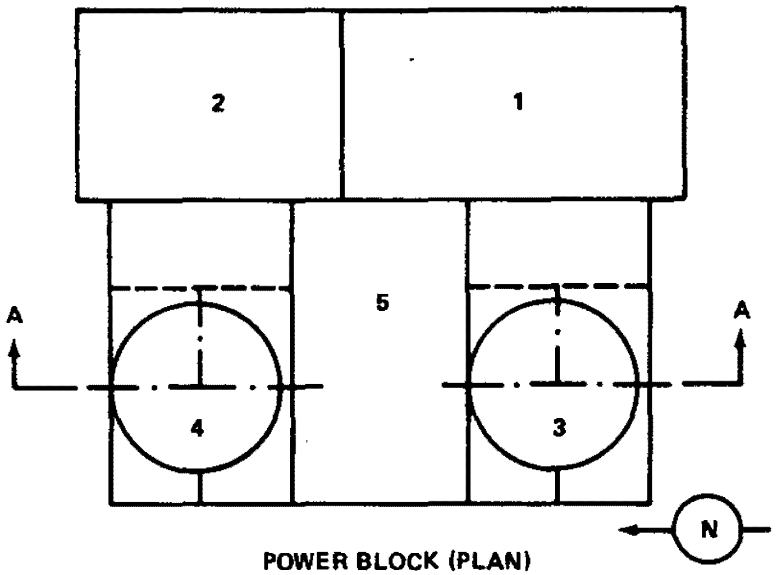

POWER BLOCK (PLAN)

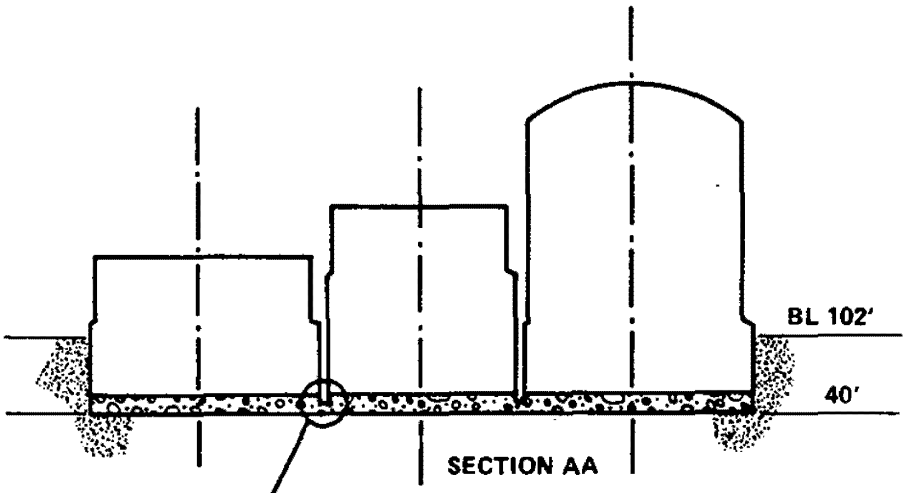

SECTION AA

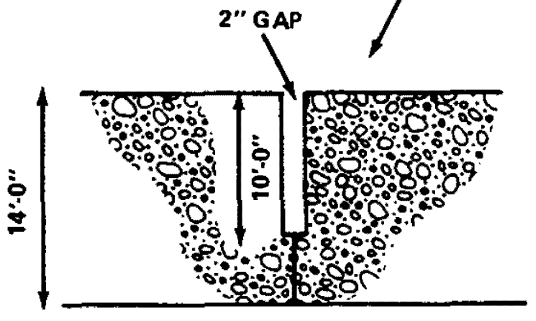

TYPICAL SEISMIC JOINT
BASE MAT

NOTE: SEE FIG. 3.8-37 FOR DESCRIPTION OF BUILDINGS

REVISION 0
APRIL 11, 1988

PUBLIC SERVICE ELECTRIC AND GAS COMPANY HOPE CREEK NUCLEAR GENERATING STATION	
POWER BLOCK LAYOUT	
UPDATED FSAR	FIGURE 3H-1

APPENDIX 3I

ULTIMATE CAPACITY OF CONTAINMENT

I. OVERVIEW

The criteria, load combinations, methodologies and results of the ultimate capacity analysis for the containment are provided in this Appendix. Figure 3.8-1 shows a sketch of the containment.

II. DESIGN CRITERIA

1. Materials

a. Containment vessel and components: SA-516 Gr. 70
Modulus of elasticity "E" (@ T = 340°F) =
27.2×10^6 psi
Tensile strength "S_u" (@ T = 340°F) = 70,000 psi

b. Bellows: SA240T304L
Modulus of elasticity "E" (@ T = 340°F) =
26.9×10^6 psi
Tensile strength "S_u" (@ T = 340°F) = 70,000 psi

Note: The above mechanical strength requirements are based on nominal stress values as specified in ASME Section III. Higher stress values may be used based on certified material test reports (CMTRS).

2. Definition of Ultimate Capacity

In accordance with discussions with NRC personnel during the NRC structural Audit on January 12, 1984, the

ultimate capacity is conservatively defined as a load which results in a stress level corresponding to the tensile strengths of the materials.

III. LOAD COMBINATIONS

The following load combination is used: D+L+P (see Table 3.8-2 for definitions). "P " is the ultimate calculated pressure.

IV. METHODOLOGY

As discussed in Section 3.8.2, the primary containment is analyzed for all loading combinations as specified in Table 3.8-2. The results of these analyses are used to obtain the stresses due to dead load (D), and live load (L). The stresses due to pressure are obtained by extrapolating the results of analyses described in Section 3.8.2. These stresses are combined and checked against the tensile strengths of the materials.

V. SUMMARY OF RESULTS

The results of the analysis are summarized in Table 3I-1.

As indicated in the table, all portions of the primary containment vessel including all components can withstand a minimum ultimate internal pressure equal to 190 psi.

The safety factor against design pressure is 3.06.

VI. REFERENCES

The following references are used in the analysis.

1. Welding Research Council, Bulletin No. 107, 1979 Revision.

2. Standards of the Expansion Joint, Manufacturers Association Inc., Fifth Edition 1980.

TABLE 3I-1

ULTIMATE INTERNAL PRESSURE SUMMARY

Description[1]	Allowable Ultimate Internal Pressure "Pa", psi	Remarks
1. Primary Containment Vessel		
a) Spherical shell	237	Effects of penetrations are included
b) Cylindrical shell	190	Effects of penetrations are included

(1) All other systems, including the suppression chamber, and components which are not included in table can withstand ultimate pressures equal to or greater than 190 psi.